

Can Multimodal LLMs Perform Time Series Anomaly Detection?

Xiongxiao Xu¹ Haoran Wang² Yueqing Liang¹ Philip S. Yu³ Yue Zhao⁴ Kai Shu²

Project Website: <https://mllm-ts.github.io>

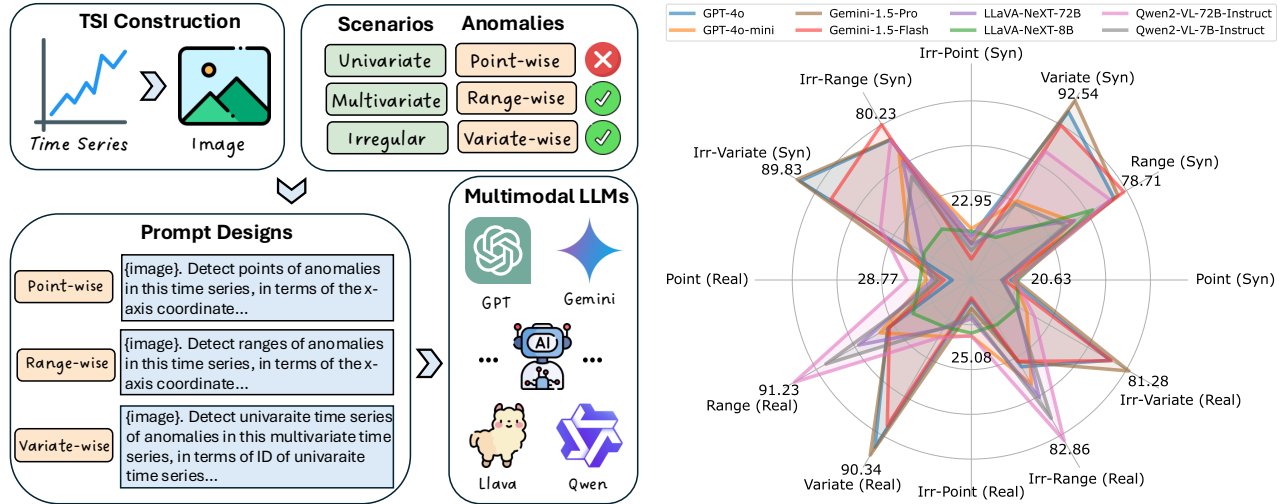


Figure 1: Left: the workflow of VISUALTIMEANOMALY. TSI: time series images. Right: the performance comparison across various setting. Varying anomaly granularities in different scenarios: *Point-wise* (Univariate), *Range-wise* (Univariate), and *Variate-wise* (Multivariate). Distinct base time series: Synthetic and Real-world. Irr: time series with irregularity.

Abstract

Large language models (LLMs) have been increasingly used in time series analysis. However, the potential of multimodal LLMs (MLLMs), particularly vision-language models, for time series remains largely under-explored. One natural way for humans to detect time series anomalies is through visualization and textual description. Motivated by this, we raise a critical and practical research question: *Can multimodal LLMs perform time series anomaly detection?* To answer this, we propose VISUALTIMEANOMALY benchmark to evaluate MLLMs in time series anomaly detection (TSAD). Our approach transforms time series numerical data into the image format and feed these images into various MLLMs, including proprietary models (GPT-4o and Gemini-1.5) and open-source models (LLaVA-NeXT and Qwen2-VL), each with one larger and one smaller vari-

ant. In total, VISUALTIMEANOMALY contains 12.4k time series images spanning 3 scenarios and 3 anomaly granularities with 9 anomaly types across 8 MLLMs. Starting with the univariate case (*point-* and *range-wise* anomalies), we extend our evaluation to more practical scenarios, including multivariate and irregular time series scenarios, and *variate-wise* anomalies. Our study reveals several key insights: 1) MLLMs detect *range-* and *variate-wise* anomalies more effectively than *point-wise* anomalies; 2) MLLMs are highly robust to irregular time series, even with 25% of the data missing; 3) open-source MLLMs perform comparably to proprietary models in TSAD. While open-source MLLMs excel on univariate time series, proprietary MLLMs demonstrate superior effectiveness on multivariate time series. Finally, we discuss the broader implications of our findings for general time series analysis in the era of MLLMs. To the best of our knowledge, this is the first work to comprehensively investigate MLLMs for TSAD, particularly for multivariate and irregular time series scenarios. We release our dataset and code at [HERE](#) to support future research.

¹Department of Computer Science, Illinois Institute of Technology, Chicago, IL, US ²Department of Computer Science, Emory University, Atlanta, GA, US ³Department of Computer Science, University of Illinois Chicago, Chicago, IL, US ⁴Department of Computer Science, University of Southern California, Los Angeles, CA, US. Correspondence to: Kai Shu <kai.shu@emory.edu>

1. Introduction

Large language models (LLMs) have gained attention across diverse applications (Kaddour et al., 2023; Ge et al., 2024), including language-based anomaly detection (Yang et al., 2024b) and time series anomaly detection (TSAD). Recent TSAD research (Liu et al., 2024c; Dong et al., 2024) shows that LLMs can provide desirable accuracy in identifying anomalies within time series. However, another study (Alnegheimish et al., 2024) reports that LLMs still lag behind traditional deep learning models by approximately 30% in performance, indicating that pure text-based LLMs may not be optimal for the challenging TSAD problem.

In parallel, progress in multimodal LLMs (MLLMs) (Yin et al., 2023) has extended LLMs to handle both visual and textual input. MLLMs represent an important step toward AGI (Artificial General Intelligence) by combining vision and language, which are two fundamental ways humans perceive and interact with the world (Huang & Zhang, 2024; Clark, 2013). Notably, MLLMs have demonstrated near-human performance on various vision-language tasks (Han et al., 2024; Wu et al., 2024; Li et al., 2023). Yet the potential of MLLMs in time series analysis has remained underexplored. In many real situations, people detect time series anomalies through a mix of visualization and language. For example, AIOps (Artificial Intelligence for IT Operations) practitioners (Li et al., 2022) interpret visual representations of metrics such as CPU usage over time and correlate them with textual information on system conditions. Motivated by this and the success of MLLMs, we pose the question: *Can multimodal LLMs perform time series anomaly detection?*

To answer this question, we propose VISUAL-TIMEANOMALY to comprehensively evaluate MLLMs in TSAD as shown in Figure 1. We convert large volumes of time series data into images, making them compatible with advanced MLLMs. Our study evaluates both proprietary models (GPT-4o (Achiam et al., 2023) and Gemini-1.5 (Team et al., 2024)) and open-source models (LLaVA-NeXT (Li et al., 2024a) and Qwen2-VL (Wang et al., 2024b)) with large-scale and relatively small model variants. We begin with the simpler univariate scenario and progress to more complex multivariate and irregular time series, reflecting real-world challenges. The anomaly granularities evolve from *point-* and *range-wise* to *variate-wise*. In total, VISUAL-TIMEANOMALY comprises 12.4k time series images spanning 3 real-world scenarios and 3 anomaly granularities with 9 anomaly types for 8 MLLMs. To the best of our knowledge, this is the first comprehensive examinations of MLLMs for TSAD, particularly for multivariate and irregular time series setting.

Key Takeaways. Our systematic exploration (Figure 1) uncovers several key findings that advance the understanding of both MLLMs and TSAD. 1) MLLMs detect *range-* and

variate-wise anomalies better than *point-wise* anomalies, suggesting that they respond better to coarse-grained patterns like humans. 2) MLLMs exhibit strong robustness to challenges posed by irregularity in time series, demonstrating that visual representations allow them to track overall patterns and detect anomalies even with 25% of data missing. 3) Open-source MLLMs perform comparably to proprietary MLLMs in TSAD. Open-source models excel in univariate scenarios, while proprietary models show more effectiveness on multivariate data.

Contributions. In summary, the paper makes the following key contributions:

- We introduce **the first comprehensive benchmark for MLLMs in TSAD**, covering diverse scenarios (univariate, multivariate, irregular) and varying anomaly granularities (*point-*, *range-*, *variate-wise*).
- We discuss several critical insights through a systematic and in-depth experimental analysis. These findings and their broader implications **significantly advance the understanding of both MLLMs and TSAD**.
- We **construct a large-scale dataset including 12.4k time series images, and release the dataset and code to the public (HERE)**, fostering future research at the intersection of MLLMs and TSAD.

2. Related Work

This work is primarily related to three lines of research (1) LLMs for time series anomaly detection, (2) time series as images, and (3) multimodal LLMs.

Time Series as Images. Time series analysis (Lee et al., 2024; Xu et al., 2024b; Du et al., 2024; Huang et al., 2024b), typically including classification, forecasting, anomaly detection, and imputation, involves multiple techniques. One recent technique is to visualize time series as image, and feed these images into powerful computer vision models for effective pattern recognition. The efforts on this area remain relatively unexplored. (Li et al., 2024b) finetunes vision transformer to perform medical classification on the time series images. (Yang et al., 2024a) and (Chen et al., 2024) utilizes vision transformer and masked autoencoder to obtain enhanced forecasting performance. The most related literature are (Zhuang et al., 2024) and (Zhou & Yu, 2024) which use MLLMs to detect anomaly detection by visualizing time series. However, they (Table 1) only focus on the univariate scenario and does not touches on variate-wise anomalies. Starting from the basic univariate scenario with point- and range-wise anomalies, our work takes the first step towards complex multivariate and irregular scenarios with variate-wise anomalies, proving the systematic exploration of MLLMs for TSAD.

LLMs for Time Series Anomaly Detection. The emergence of LLMs brings new paradigms for TSAD, especially in data-efficient scenarios. (Liu et al., 2024a) regards LLMs

Work	Univariate	Multivariate	Irregular	Point	Range	Variate
(Zhou & Yu, 2024)	✓	✗	✗	✗	✓	✗
(Zhuang et al., 2024)	✓	✗	✗	✓	✓	✗
Ours	✓	✓	✓	✓	✓	✓

Table 1: Comparison between our work and the existing two works that utilize MLLMs for TSAD.

as a teacher network to guide training of the prototype-based Transformer student network. (Liu et al., 2024c; Dong et al., 2024) employs in-context learning and chain-of-thought to mimic expert logic for enhanced anomaly detection performance. The above work indicates promising performance of LLMs in TSAD. However, the later work (Alnegheimish et al., 2024) shows LLMs-based methods are still inferior to traditional SOTA deep learning models by 30% on F1-Score. It suggests TSAD still remains a challenging task for LLMs which are pre-trained on only language. Additionally, (Zhou & Yu, 2024) and (Dong et al., 2024) indicate that the visual representation of time series facilitates anomaly detection, which demonstrates further the importance of transforming time series into images. Different from the existing work, our study takes the first attempt to comprehensively examine the potential of MLLMs for TSAD, covering univariate, multivariate, and irregular scenarios with point-, range- and variate-wise anomalies.

Multimodal LLMs. Multimodal large language models (MLLMs) (Yin et al., 2023) refer to LLMs-based models with the ability to process multimodal information, such as text (Liang et al., 2024; Huang et al., 2024a), images (Liu et al., 2024b; Hu et al., 2024), audio (Deshmukh et al., 2023; Zhang et al., 2023), and video (He et al., 2024; Fu et al., 2024), and table (Sui et al., 2024; Wang et al., 2024a). A significant amount of endeavors (Hilal et al., 2022; Black et al., 2024) have been put into grounding natural languages and visual images in MLLMs, i.e., vision-language models. According to accessibility of code, MLLMs can be categorized into two classes: propriety and open-source. Proprietary MLLMs are not publicly accessible but can be utilized via APIs provided by companies, consisting of GPT-4 (Achiam et al., 2023), Gemini-1.5 (Team et al., 2024), etc. In contrast, open-source MLLMs allow researchers and developers to access and modify the codes, subject to the terms of their respective licenses, including LLaVA-NeXT (Li et al., 2024a) and Qwen2-VL (Wang et al., 2024b), etc. Compared to numerous vision-language models, the alignment among vision, language, and time series is significantly less explored. Our work gives an intuitive way to bridge image, text, and time series into MLLMs.

3. VISUALTIMEANOMALY: Time Series Anomaly Detection based on Image

We present VISUALTIMEANOMALY, a new image-based TSAD benchmark that covers univariate, multivariate, and irregular time series. First, we define time series anomalies

at different granularities across these scenarios. Next, we outline the methodology for constructing time series images. We finally describe utilized MLLMs, prompts, and metrics.

3.1. Time Series Scenarios

This work begins with base time series and then considers three common types in practice (Zamanzadeh Darban et al., 2024): univariate, multivariate, and irregular time series. **Base time series** is the starting point for all scenarios. It is assumed to follow either an explicit or an implicit generative function $G(x)$. An explicit generative function has a closed-form expression (e.g., *sine* and *cosine* waves). An implicit generative function captures complex real-world time series (Dau et al., 2019; Bagnall et al., 2018) that lack a definitive functional form. Both types are used to generate univariate, multivariate, and irregular time series.

Univariate time series is a sequence of values over time, denoted as $\mathbf{x} = \{x_1, x_2, \dots, x_T\}$ with T timestamps, where $x_t \in \mathbb{R}$ represents the value at the t^{th} timestamp. For the explicit generative function, we use *sine* waves, and for the implicit one, we use the Symbols dataset from the UCR archive (Dau et al., 2019).

Multivariate time series carries multiple features at a timestamp. Formally, a multivariate time series can be denoted as $\mathbf{X} = \{\mathbf{x}^1, \mathbf{x}^2, \dots, \mathbf{x}^M\}$ with M variables, where $\mathbf{x}^m \in \mathbb{R}^T$ is a T -dimensional vector at the m^{th} variate. The multivariate time series \mathbf{X} can also be expressed as $\mathbf{X} = \{\mathbf{x}_1, \mathbf{x}_2, \dots, \mathbf{x}_T\}$ with T timestamps, where $\mathbf{x}_t \in \mathbb{R}^M$ carries M features at the t^{th} timestamp. The explicit generative function adopts *sine* and *cosine* waves, and the implicit generative function adopts the ArticulatoryWordRecognition dataset in the UEA time series multivariate archive (Bagnall et al., 2018).

Irregular time series refers to univariate/multivariate time series with irregular sampled data points, which naturally arises in domains such as biology and healthcare (Shukla & Marlin, 2020). Formally, an irregular univariate time series can be represented as $\mathbf{x}_{irr} = \{x_1, \dots, x_{i-1}, x_{i+2}, \dots, x_T\}$ with S ($S < T$) timestamps, where the point x^i at the i^{th} timestamp is missing. Similarly, an irregular multivariate time series is $\mathbf{X}_{irr} = \{\mathbf{x}_{irr}^1, \mathbf{x}_{irr}^2, \dots, \mathbf{x}_{irr}^M\}$, where \mathbf{x}_{irr}^m is a S -dimensional vector at the m^{th} variate. We define the irregularity ratio as $r = 1 - \frac{S}{T}$ for irregular univariate/multivariate time series scenarios. We obtain the irregular univariate/multivariate scenario by randomly dropping data points for the above univariate/multivariate time series.

3.2. Anomaly Definition

In this subsection, we define time series anomalies of varying granularities in univariate and multivariate time series, including *point-wise*, *range-wise*, and *variate-wise* anomalies, and introduce these in the irregular scenario.

As shown in Figure 2(a), univariate time series anomalies can be classified into *point-wise* and *range-wise* anomalies.

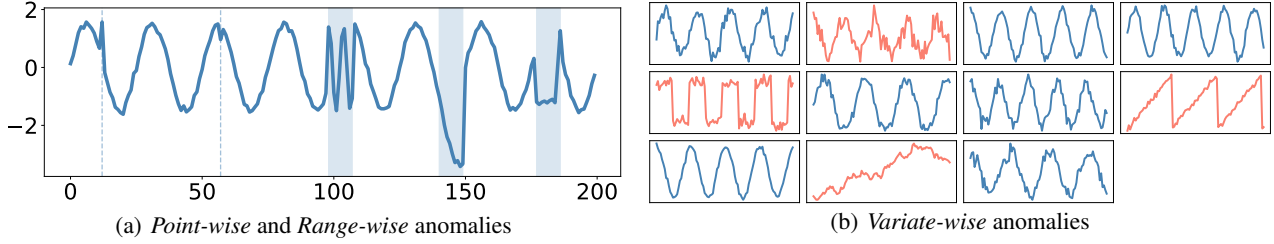


Figure 2: The illustration of *point-wise*, *range-wise*, and *variate-wise* anomalies. In Figure 2(a), dashed lines and highlighted intervals represent global, contextual, seasonal, trend, and shapelet anomalies, respectively, from left to right. Figure 2(b) illustrates *variate-wise* anomalies (and the construction of multivariate time series images). From left to right and top to bottom, time series marked by the red color indicate triangle, square, sawtooth, and random anomalies, respectively.

lies (Zamanzadeh Darban et al., 2024; Lai et al., 2021).

Point-wise anomalies are defined as unexpected incidents at individual time points:

$$|x_t - \hat{x}_t| > \delta \quad (1)$$

where \hat{x}_t is the expected value at timestamp t , which can be the output of a regression model, or the global mean value or mean value of a context window, and δ is the threshold.

Global anomalies are data points that significantly deviate from the rest of the series. They are usually spikes or dips in time series. The threshold can be defined as $\delta = \lambda \cdot \sigma(\mathbf{x})$, where $\sigma(\mathbf{x})$ is the standard deviation of the time series and λ controls the threshold level.

Contextual anomalies refer to the points that deviate from the neighboring time points within certain ranges. They exist usually in the form of small glitches in time series. The threshold $\delta = \lambda \cdot \sigma(\mathbf{x}_{t-k:t+k})$, where $\mathbf{x}_{t-k:t+k}$ is the context window of the data points x_t with size k .

Range-wise anomalies represent anomalous subsequences characterized by changes in seasonality, trend, or shape. Formally, within a time series \mathbf{x} , an underlying subsequence $\mathbf{x}_{i:j}$ from timestamp i to j can be considered anomalous if:

$$\text{diss}(\mathbf{x}_{i:j}, \hat{\mathbf{x}}_{i:j}) > \delta \quad (2)$$

where diss is a function measuring the dissimilarity between two subsequences regarding to seasonality, trend or shape, such as dynamic time warping (Berndt & Clifford, 1994), and $\hat{\mathbf{x}}_{i:j}$ is the expected subsequence regarding to seasonality, trend or shapelet.

Seasonal anomalies are subsequences with unusual seasonalities compared to the overall seasonality, despite the normal trends and shapes of time series.

Trend anomalies refer to subsequences which significantly alter the trend of the time series while retaining basic shapelet and seasonality.

Shapelet anomalies indicate the subsequences with dissimilar basic shapelet compared with the normal shapelet.

Figure 2(b) illustrates *variate-wise* anomalies of the multivariate time series scenario. In multivariate time series images, we only focus on *variate-wise* anomalies as finer-granularity anomalies are too subtle for MLLMs and even

human to detect.

Variate-wise anomalies are the entire time series of some variates which significantly deviate from other variates within multivariate time series. We assume each variate m is governed by a generative function $G(x)_m$. We define the *variate-wise* anomalies as follows:

$$\text{diss}(G(x)_m, \hat{G}(x)_m) > \delta \quad (3)$$

where diss is utilized to measure the dissimilarity between two sequences of univariate time series, and $\hat{G}(x)_m$ denotes the expected generative function or the majority generative functions among variates, such as *sine* or *cosine* waves.

Triangle anomalies denote variates exhibiting the anomalous behavior that follows a triangular wave pattern, with linear ascents and descents.

Square anomalies are anomalous sequences whose anomalies manifest as abrupt transitions between high and low states, forming a square wave pattern.

Sawtooth anomalies refer to variates displaying periodic anomalies with a gradual rise and a sharp drop, characteristic of a sawtooth wave.

Random anomalies are variates driven by stochastic processes, exhibiting erratic changes of a random walk.

Irregular anomalies are defined based on the irregular univariate/multivariate time series. To introduce irregularity, we randomly drop data points in univariate/multivariate time series, leading to irregular anomalies. For univariate time series, we skip contextual anomalies as dropping points around the anomalies will damage the context window. We also exclude seasonal anomalies when base time series employs an implicit generative function, as determining the seasonalities of real-world time series dataset (such as Symbol dataset) is challenging.

3.3. Time Series Images Construction

One crucial element of enabling MLLMs to detect time series anomalies lies in the construction of time series images (TSI). In this subsection, we detail the process of transforming numerical time series data into corresponding TSI.

Univariate TSI Construction. We first inject two types of *point-wise* anomalies and three types of *range-wise* anomalies into univariate time series. Then we convert them into

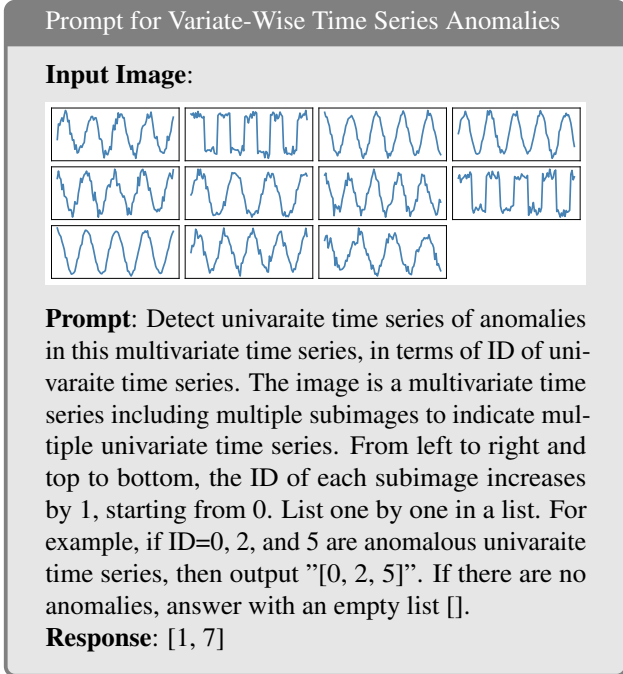


Figure 3: The prompt for *variate-wise* anomalies.

the image format with the x-axis helping MLLMs identify the positions of anomalies. As shown in Figure 2(a), we derive five types of univariate TSI datasets corresponding to five anomaly categories: global, contextual, seasonal, trend, and shapelet. Each type of dataset consists of 100 different TSI with varying noise.

Multivariate TSI Construction. The construction of multivariate TSI is non-trivial considering the multiple dimensions of time series and limited input context of MLLMs. To effectively represent multivariate time series in a single image, we convert each variable of a multivariate time series into a subimage, and arrange these subimages in a grid format. This concise representation allows MLLMs to capture inter-variable correlations within a single image. We omit coordinate axes as they are not crucial for detecting *variate-wise* anomalies, which emphasize deviations in the overall patterns of time series. Specifically, we place M variables of a multivariate time series in a grid of size $n \times n$ if $n \times (n - 1) < M \leq n \times n$, or a grid of size $n \times (n + 1)$ if $n \times n < M \leq n \times (n + 1)$. We leave a blank if there exists extra spaces ($M < n \times n$ or $M < n \times (n + 1)$). For example, a multivariate time series with 9 variates is arranged in a grid of 3×3 ; a 11-variates time series is arranged in a grid of 3×4 , with an additional subimage blank. Figure 2(b) illustrates an example of 11-variates time series.

We synthesize four types of multivariate TSI datasets corresponding to four *variate-wise* anomaly types: triangle, square, sawtooth, and random. Each dataset comprises of 100 multivariate TSI with varying noise.

Irregular TSI Construction. We build irregular TSI datasets by inheriting from the univariate/multivariate TSI

datasets. We randomly omit data points in the univariate/multivariate TSI datasets, and leave the omitted points blank in the visualization.

Examples of univariate, multivariate, and irregular time series images can be found in Appendix D.

3.4. Multimodal LLMs, Prompts, and Metrics

In this subsection, we introduce the adopted multimodal LLMs, prompts, and evaluation metrics.

Multimodal LLMs. We conduct experiments on the representative multimodal LLMs, including both proprietary and open-source MLLMs. For each MLLM family, we select one larger and one smaller model to ensure a comprehensive evaluation. The proprietary models include GPT-4 (GPT-4o and GPT-4o mini) and Gemini-1.5 (Gemini-1.5-pro and Gemini-1.5-flash); the open-source models consist of LLaVA-NeXT (LLaVA-NeXT-72B and LLaVA-NeXT-8B) and Qwen2-VL (Qwen2-VL-72B-Instruct and Qwen2-VL-7B-Instruct). The details of the MLLMs are in Appendix A.

Prompts. We design different prompts for *point-*, *range-*, and *variate-wise* anomalies, respectively. We illustrate the prompt example for *variate-wise* anomalies in Figure 3 as the prompt is more challenging for MLLMs to understand. Other prompt examples can be found in Appendix B.

Evaluation Metrics. The performance of TSAD is commonly quantified by precision, recall, and F1 score (Lai et al., 2021). However, (Huet et al., 2022) emphasizes these metrics are unaware of the temporal adjacency and events durations within time series. Instead, for *point-wise* and *range-wise* anomalies, we report precision, recall, and F1 score based on the concept of affiliation as defined in (Huet et al., 2022) for robust evaluation. For *variate-wise* anomalies, we employ vanilla precision, recall, and F1 score to assess MLLMs because *variate-wise* anomalies do not involve temporal adjacency or events durations among variates. We report them in the format of percentage in the discussion.

4. Results and Analysis

4.1. Scenario 1: Univariate Time Series

The univariate time series represents a fundamental scenario in TSAD, where observations are sequentially recorded for a single variable over time. Despite its simplicity, it serves as a critical foundation for assessing MLLM performance before addressing more complex situations.

Table 2 and Table 3 compare the MLLMs across *point-* and *range-wise* anomalies, respectively. Accordingly, we have the following observations:

Range-wise anomalies are easier to detect than point-wise anomalies. Specifically, the ranking of anomaly categories w.r.t. detection performance is: *trend* > *shapelet* > *seasonal* > *global* > *contextual*. The former three are *range-wise*, and the latter two belong to *point-wise*. For example, GPT-4o obtains recall score 72.47, 68.86, 54.11, 13.19, and 2.91 on trend, shapelet, seasonal, global,

Table 2: Performance on *point-wise* anomalies. The best and the second best performance are bold and underlined.

Base Time Series Anomaly Type Evaluation Metrics	<i>Sine</i>						Symbols					
	Global			Contextual			Global			Contextual		
	P	R	F1									
GPT-4o	55.71	<u>13.19</u>	17.91	19.26	2.91	4.66	26.97	5.95	8.53	4.67	0.92	1.30
GPT-4o-mini	41.03	12.85	19.09	23.84	9.17	12.99	44.10	13.79	20.07	27.94	11.26	15.04
Gemini-1.5-Pro	62.00	12.37	19.76	45.27	6.05	10.38	48.67	9.62	15.30	41.52	5.05	8.73
Gemini-1.5-Flash	<u>58.57</u>	8.67	14.79	21.41	1.82	3.32	<u>49.84</u>	7.16	12.21	17.54	1.54	2.78
LLaVA-NeXT-72B	46.26	8.64	14.01	45.82	4.26	7.68	47.92	10.90	17.33	46.56	10.91	17.33
LLaVA-NeXT-8B	52.06	12.96	20.63	<u>49.51</u>	11.38	18.48	47.86	<u>15.42</u>	<u>22.94</u>	46.56	<u>13.89</u>	<u>20.85</u>
Qwen2-VL-72B-Instruct	51.79	13.44	<u>19.93</u>	51.15	<u>10.51</u>	<u>16.80</u>	51.64	23.89	28.77	51.71	29.92	33.04
Qwen2-VL-7B-Instruct	47.77	8.02	13.68	49.16	7.77	13.19	45.27	8.47	14.13	<u>47.00</u>	9.21	14.92

Table 3: Performance on *range-wise* anomalies. The best and the second best performance are bold and underlined.

Base Time Series Anomaly Type Evaluation Metrics	<i>Sine</i>									Symbols					
	Seasonal			Trend			Shapelet			Trend			Shapelet		
	P	R	F1												
GPT-4o	55.54	54.11	52.89	<u>80.13</u>	72.47	73.48	82.50	68.86	<u>72.92</u>	50.29	42.03	44.28	43.23	32.86	36.19
GPT-4o-mini	15.93	22.99	18.38	48.72	61.52	52.32	44.96	60.88	50.11	50.27	60.33	52.58	47.18	68.02	54.06
Gemini-1.5-Pro	50.36	45.51	46.27	78.67	<u>78.51</u>	<u>75.60</u>	78.34	66.51	69.87	53.36	48.90	48.88	42.72	33.78	36.34
Gemini-1.5-Flash	34.26	31.17	31.79	86.86	76.10	78.71	78.72	<u>70.48</u>	72.59	54.87	44.58	47.59	42.27	34.16	36.57
LLaVA-NeXT-72B	35.44	39.95	36.15	53.11	57.22	53.29	35.81	33.80	33.55	57.00	57.83	55.55	58.11	68.18	61.11
LLaVA-NeXT-8B	<u>55.30</u>	<u>51.92</u>	<u>51.62</u>	52.75	83.35	62.58	51.37	60.10	53.21	7.84	11.92	8.99	30.04	53.24	37.90
Qwen2-VL-72B-Instruct	24.44	26.27	24.92	78.32	70.82	71.63	<u>80.66</u>	79.24	78.32	86.98	<u>80.17</u>	81.10	91.23	94.28	92.19
Qwen2-VL-7B-Instruct	38.99	43.06	40.20	51.61	49.31	48.59	23.62	27.13	24.75	<u>73.63</u>	84.83	<u>77.56</u>	<u>75.08</u>	81.76	<u>77.70</u>

Table 4: Performance on *variate-wise* anomalies ($M = 9$) reported in Precision and F1. The best and the second best performance are bold and underlined. The complete results are in Appendix E.

Base Time Series Anomaly Type Evaluation Metrics	Sine/Cosine								Articulatory Word Recognition							
	Triangle		Square		Sawtooth		Random		Triangle		Square		Sawtooth		Random	
	P	F1	P	F1	P	F1	P	F1	P	F1	P	F1	P	F1	P	F1
GPT-4o	<u>39.59</u>	<u>47.12</u>	56.88	63.28	43.02	53.58	<u>84.52</u>	<u>86.79</u>	46.99	54.59	<u>81.93</u>	<u>86.18</u>	43.54	48.54	<u>23.05</u>	27.64
GPT-4o-mini	8.46	11.82	20.68	27.82	8.13	11.26	32.92	40.79	18.19	28.35	19.23	29.08	17.13	26.56	16.78	26.15
Gemini-1.5-Pro	53.05	51.15	81.42	82.52	80.25	80.47	92.07	92.54	60.92	66.81	87.92	90.34	73.09	79.17	13.66	16.37
Gemini-1.5-Flash	37.57	39.21	<u>70.58</u>	<u>70.70</u>	<u>62.67</u>	<u>61.94</u>	81.67	79.94	<u>51.86</u>	<u>55.87</u>	70.26	75.15	<u>67.42</u>	<u>73.44</u>	23.83	24.82
LLaVA-NeXT-72B	15.24	23.20	16.38	24.66	14.06	21.36	18.66	25.27	19.10	28.01	16.34	25.06	15.58	23.74	18.01	26.86
LLaVA-NeXT-8B	15.25	22.19	15.25	22.19	15.25	22.19	15.08	21.99	16.05	21.14	17.87	24.14	15.80	21.29	17.26	22.85
Qwen2-VL-72B-Instruct	32.57	37.49	29.48	35.57	36.73	40.67	64.83	66.27	18.47	23.45	23.69	29.90	22.10	27.93	12.93	16.54
Qwen2-VL-7B-Instruct	21.79	22.32	26.87	29.00	20.04	21.68	39.69	39.22	19.32	24.50	19.32	24.50	19.32	24.50	19.32	24.50

and contextual, respectively, for *sine* waves as base time series. The primary reason is that *range-wise* anomalies, consisting of sequences of point anomalies that significantly deviate from normal patterns, are more distinguishable than dispersed *point-wise* anomalies. This observation is further supported by Figure 2(a).

Open-source MLLMs outperform proprietary models in detecting *point-wise* and *range-wise* anomalies. Qwen2-VL-72B-Instruct, the SOTA open-source MLLM, achieves the highest or second-highest F1 score on *point-wise* anomalies and demonstrates comparable or superior effectiveness to other MLLMs across most *range-wise* anomalies. For example, when base time series employs Symbols dataset, Qwen2-VL-72B-Instruct attains F1 scores of 28.77, 33.04, 81.10, and 92.19 on global, contextual, trend, and shapelet anomalies, respectively, outperforming all other MLLMs. **Real-world time series does not increase the difficulty of**

time series anomaly detection. We do not observe significant performance degradation when base time series transitions from classical *sine* waves to the real-world dataset. For instance, GPT-4o family and Gemini-1.5 family exhibit reduced effectiveness, whereas Qwen2-VL family shows improved performance in detecting trend and shapelet anomalies when shifting from *sine* waves to real-world dataset.

Insight 1: (1) MLLMs are more effective at detecting coarse-granularity (*range-wise*) than fine-granularity (*point-wise*) anomalies in univariate time series; (2) Open-source MLLMs outperform proprietary models in the univariate scenario.



Figure 4: The impact of number of dimensions M on MLLMs for *variate-wise* anomalies

4.2. Scenario 2: Multivariate Time Series

Multivariate time series is composed of multiple variables (features) recorded over time. Unlike univariate time series, which tracks a single variable, multivariate time series involve multiple interdependent variables that may influence or correlate with each other. Multivariate time series is ubiquitous in real-world applications such as urban analytics (Tabassum et al., 2021), scientific computing (Xu et al., 2024a), and climate modeling (Zhu et al., 2023). For example, in climate modeling, the recorded features might consist of temperature, humidity, wind speed, and rainfall observed at regular time intervals like hourly or daily.

Table 4 compares MLLMs on *variate-wise anomalies*. We observe the below findings:

The *variate-wise* anomalies can be generally identified by MLLMs. The SOTA MLLM, Gemini-1.5-Pro, is capable of achieving the maximum F1 score 92.54 and 90.34 on synthetic and real-world dataset, respectively. The impressive results demonstrates that MLLMs can capture inter-variables relationship in multivariate TSI and thus lead to enhanced detection performance. It also suggests that, compared to *point-* and *range-wise*, *variate-wise* anomalies can be detected with the highest performance as they exhibit the coarsest granularity.

Proprietary MLLMs are superior to open-source models in detecting *variate-wise* anomalies. We clearly observe that almost all the best and the second best performance lies in the proprietary MLLMs. It indicates that proprietary models are capable of understanding multivariate TSI and capturing inter-variable relationship, leading to enhanced anomaly detection performance.

The detection of *variate-wise* anomalies heavily depends on patterns of the majority of variables within a multivariate time series. On time series governed by *sinelcosine* waves, Gemini-1.5-Pro attains the highest F1 score 92.54 for random anomalies. However, for the same anomaly type in real-world time series, its performance drops significantly to an F1 score of 16.37. This discrepancy arises as the random walk pattern deviates substantially from *sinelcosine* waves,

whereas most time series in the ArticularyWordRecognition dataset closely resemble a random walk.

Impact of Variates M . We also investigate the impact of the number of variates M in multivariate TSI. Intuitively, as M increases, the information density that MLLMs must process grows. Moreover, this comes at the cost of reduced resolution for each subimage (variate). Consequently, **the effectiveness of MLLMs decreases as M increases.** Figure 4 illustrates this effect, showing a gradual decline in detection performance from $M = 4$ to $M = 36$, which aligns with our intuition. For instance, Gemini-1.5-Pro achieves an impressive F1 score of 100 at $M = 4$, but this drops significantly to 33.2 when $M = 36$.

Hallucination. We find that MLLMs, particularly small-scale open-source models such as LLaVA-NeXT-8B and Qwen2-VL-7B-Instruct, are prone to generating hallucinated responses when handling multivariate TSI. For example, when given a 9-dimensional time series as input, LLaVA-NeXT-8B may produce an ungrounded sequence such as "[0, 1, 2, ..., 100, 101, 102, ...]" until reaching the maximum token limit. This hallucination arises because prompts for *variate-wise* anomalies pose significantly greater challenges to MLLMs' comprehension capabilities compared to *point-* and *range-wise* anomalies. Small-scale open-source models, in particular, often fail to fully grasp the complexity of such prompts.

Insight 2: (1) MLLMs generally can effectively detect *variate-wise* anomalies in multivariate time series. (2) Proprietary MLLMs outperform open-source models in the multivariate scenario. (3) MLLMs are sensitive to dimensionality and can generate hallucination for multivariate time series.

4.3. Scenario 3: Irregular Time Series

Irregular time series are characterized by unevenly spaced observations. Unlike regular time series, which assume consistent sampling intervals, irregular time series naturally

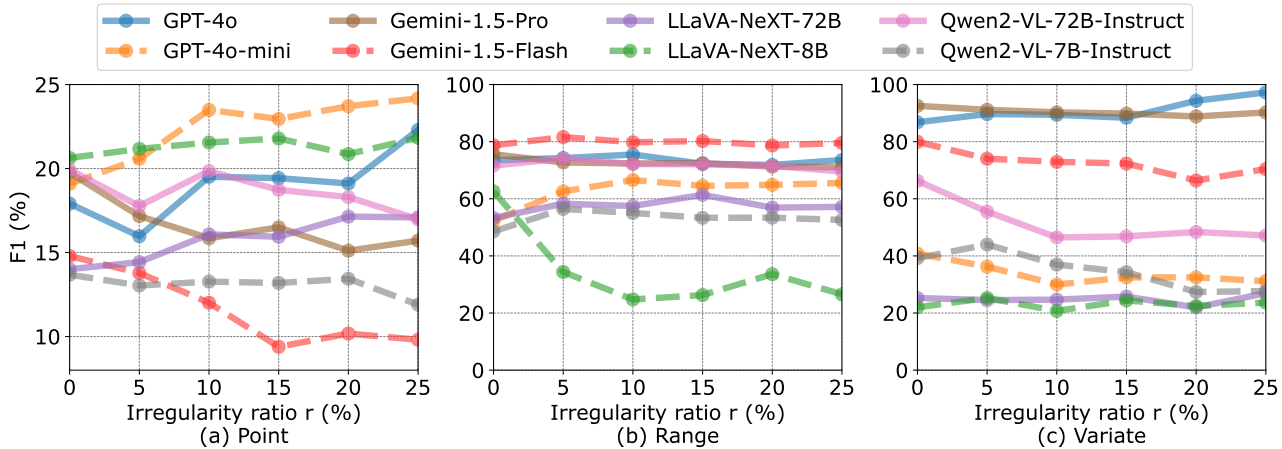


Figure 5: The impact of the irregularity ratio r on MLLMs for *point-wise*, *range-wise*, and *variate-wise* anomalies.

arise in domains where data collection is influenced by external factors. For instance, in healthcare domain (Li et al., 2024b), sensor readings from wearable devices may be recorded at irregular intervals due to the patient activity or device connectivity. These irregularities pose unique challenges for traditional time series analysis, as standard techniques often assume fixed sampling rates.

We conduct irregular time series experiments by changing the irregularity ratio r from 5% to 25%. Figure 5 compares MLLMs on irregular univariate/multivariate time series.

We clearly observe that **MLLMs exhibit strong robustness against the challenges posed by irregularity**. Irregular time series, characterized by inherent inconsistencies, are often more challenging and can degrade the performance of traditional TSAD algorithms. However, MLLMs effectively mitigate the negative effects of irregularity by representing the entire time series with leaving missed values blank. This intuitive visualization approach preserves the overall patterns of time series, enabling MLLMs to detect anomalies. For example, on *point-wise* anomalies, the maximum performance degradation (Gemini-1.5-Flash) among all MLLMs is only a 4.89 decrease of F1 score. This result underscores the effectiveness of visualization and capability of MLLMs to handle time series irregularities.

Insight 3: Visualizing time series as images is a highly effective way to represent irregular time series. This approach enables MLLMs to demonstrate strong robustness against challenges posed by irregularity.

5. Implications on Time Series Anomaly Detection in the Era of Multimodal LLMs

Our empirical analysis have key implications on TSAD and general time series tasks in the era of multimodal LLMs.

First, our findings imply that **MLLMs excel at identifying broader patterns and dependencies within time series data**. This capability is crucial for applications where anomalies manifest as broader patterns such as financial market trends. Second, the robustness of MLLMs to irregular time series, even with significant data dopped, highlights that **MLLMs have great potential in real-world applications with compromised data quality**. This resilience makes MLLMs a viable option for domains like healthcare, IoT, and environmental monitoring, where missing or irregularly sampled data is common. Finally, **there is a paradigm shift of time series tasks from numerical data into multimodal format**. By integrating multimodal capabilities, models can understand multimodal information (e.g., text, images, or domain knowledge) to enhance detection accuracy. We call for future research to explore how multimodal inputs can be further leveraged to improve not only time series anomaly detection but also general time series tasks such as forecasting, classification, and imputation.

6. Conclusion and Future Work

In this paper, we address the research question: *Can multimodal LLMs perform time series anomaly detection?* We introduce a novel image-based benchmark, VISUAL-TIMEANOMALY, which provides a comprehensive evaluation of MLLMs for TSAD, offering valuable insights into their strengths and limitations across diverse scenarios. Our findings reveal several key insights: 1) MLLMs exhibit stronger capabilities in detecting *range-* and *variate-wise* anomalies than *point-wise* anomalies; 2) MLLMs demonstrate robustness against the irregularity of time series; 3) open-source models excel in univariate scenarios, whereas proprietary models perform more effectively on multivariate data. Our work paves the way for further research at the intersection of MLLMs and time series analysis.

Despite these valuable contributions, we encounter challenges that inspire future research. For instance, small-scale

open-source MLLMs such as LLaVA-NeXT-8B exhibit a tendency to generate hallucinations for multivariate time series. Mitigating hallucinations of MLLMs for time series anomaly detection presents an exciting research direction. Moreover, exploring more effective approaches to visualize time series as images, particularly for high-dimensional multivariate time series is promising.

Impact Statement

This paper presents work whose goal is to advance the field of multimodal LLMs and time series analysis. There are many potential societal consequences of our work, none of which we feel must be specifically highlighted here.

References

- Achiam, J., Adler, S., Agarwal, S., Ahmad, L., Akkaya, I., Aleman, F. L., Almeida, D., Altenschmidt, J., Altman, S., Anadkat, S., et al. Gpt-4 technical report. *arXiv preprint arXiv:2303.08774*, 2023.
- Alnegheimish, S., Nguyen, L., Berti-Equille, L., and Veeramachaneni, K. Large language models can be zero-shot anomaly detectors for time series? *arXiv preprint arXiv:2405.14755*, 2024.
- Bagnall, A., Dau, H. A., Lines, J., Flynn, M., Large, J., Bostrom, A., Southam, P., and Keogh, E. The uea multivariate time series classification archive, 2018. *arXiv preprint arXiv:1811.00075*, 2018.
- Berndt, D. J. and Clifford, J. Using dynamic time warping to find patterns in time series. In *Proceedings of the 3rd international conference on knowledge discovery and data mining*, pp. 359–370, 1994.
- Black, K., Brown, N., Driess, D., Esmail, A., Equi, M., Finn, C., Fusai, N., Groom, L., Hausman, K., Ichter, B., et al. A vision-language-action flow model for general robot control. *arXiv preprint arXiv:2410.24164*, 2024.
- Chen, M., Shen, L., Li, Z., Wang, X. J., Sun, J., and Liu, C. Visionts: Visual masked autoencoders are free-lunch zero-shot time series forecasters. *arXiv preprint arXiv:2408.17253*, 2024.
- Clark, A. Whatever next? predictive brains, situated agents, and the future of cognitive science. *Behavioral and brain sciences*, 36(3):181–204, 2013.
- Dau, H. A., Bagnall, A., Kamgar, K., Yeh, C.-C. M., Zhu, Y., Gharghabi, S., Ratanamahatana, C. A., and Keogh, E. The ucr time series archive. *IEEE/CAA Journal of Automatica Sinica*, 6(6):1293–1305, 2019.
- Deshmukh, S., Elizalde, B., Singh, R., and Wang, H. Pengi: An audio language model for audio tasks. *Advances in Neural Information Processing Systems*, 36:18090–18108, 2023.
- Dong, M., Huang, H., and Cao, L. Can llms serve as time series anomaly detectors? *arXiv preprint arXiv:2408.03475*, 2024.
- Du, W., Wang, J., Qian, L., Yang, Y., Ibrahim, Z., Liu, F., Wang, Z., Liu, H., Zhao, Z., Zhou, Y., et al. Tsi-bench: Benchmarking time series imputation. *arXiv preprint arXiv:2406.12747*, 2024.
- Fu, C., Dai, Y., Luo, Y., Li, L., Ren, S., Zhang, R., Wang, Z., Zhou, C., Shen, Y., Zhang, M., et al. Video-mme: The first-ever comprehensive evaluation benchmark of multi-modal llms in video analysis. *arXiv preprint arXiv:2405.21075*, 2024.
- Ge, Y., Hua, W., Mei, K., Tan, J., Xu, S., Li, Z., Zhang, Y., et al. Openagi: When llm meets domain experts. *Advances in Neural Information Processing Systems*, 36, 2024.
- Han, T., Adams, L. C., Bressemer, K. K., Busch, F., Nebelung, S., and Truhn, D. Comparative analysis of multimodal large language model performance on clinical vignette questions. *JAMA*, 2024.
- He, B., Li, H., Jang, Y. K., Jia, M., Cao, X., Shah, A., Shrivastava, A., and Lim, S.-N. Ma-lmm: Memory-augmented large multimodal model for long-term video understanding. In *Proceedings of the IEEE/CVF Conference on Computer Vision and Pattern Recognition*, pp. 13504–13514, 2024.
- Hilal, W., Gadsden, S. A., and Yawney, J. Financial fraud: a review of anomaly detection techniques and recent advances. *Expert systems With applications*, 193:116429, 2022.
- Hu, W., Xu, Y., Li, Y., Li, W., Chen, Z., and Tu, Z. Bliva: A simple multimodal llm for better handling of text-rich visual questions. In *Proceedings of the AAAI Conference on Artificial Intelligence*, volume 38, pp. 2256–2264, 2024.
- Huang, B., Chen, C., Xu, X., Payani, A., and Shu, K. Can knowledge editing really correct hallucinations? *arXiv preprint arXiv:2410.16251*, 2024a.
- Huang, J. and Zhang, J. A survey on evaluation of multimodal large language models. *arXiv preprint arXiv:2408.15769*, 2024.

- Huang, X., Chen, W., Hu, B., and Mao, Z. Graph mixture of experts and memory-augmented routers for multivariate time series anomaly detection. *arXiv preprint arXiv:2412.19108*, 2024b.
- Huet, A., Navarro, J. M., and Rossi, D. Local evaluation of time series anomaly detection algorithms. In *Proceedings of the 28th ACM SIGKDD Conference on Knowledge Discovery and Data Mining*, pp. 635–645, 2022.
- Kaddour, J., Harris, J., Mozes, M., Bradley, H., Raileanu, R., and McHardy, R. Challenges and applications of large language models. *arXiv preprint arXiv:2307.10169*, 2023.
- Lai, K.-H., Zha, D., Xu, J., Zhao, Y., Wang, G., and Hu, X. Revisiting time series outlier detection: Definitions and benchmarks. In *Thirty-fifth conference on neural information processing systems datasets and benchmarks track (round 1)*, 2021.
- Lee, Z., Lindgren, T., and Papapetrou, P. Z-time: efficient and effective interpretable multivariate time series classification. *Data mining and knowledge discovery*, 38(1): 206–236, 2024.
- Li, B., Wang, R., Wang, G., Ge, Y., Ge, Y., and Shan, Y. Seed-bench: Benchmarking multimodal llms with generative comprehension. *arXiv preprint arXiv:2307.16125*, 2023.
- Li, B., Zhang, K., Zhang, H., Guo, D., Zhang, R., Li, F., Zhang, Y., Liu, Z., and Li, C. Llava-next: Stronger llms supercharge multimodal capabilities in the wild, May 2024a. URL <https://llava-vl.github.io/blog/2024-05-10-llava-next-stronger-llms/>.
- Li, Z., Zhao, N., Zhang, S., Sun, Y., Chen, P., Wen, X., Ma, M., and Pei, D. Constructing large-scale real-world benchmark datasets for aiops. *arXiv preprint arXiv:2208.03938*, 2022.
- Li, Z., Li, S., and Yan, X. Time series as images: Vision transformer for irregularly sampled time series. *Advances in Neural Information Processing Systems*, 36, 2024b.
- Liang, Y., Yang, L., Wang, C., Xu, X., Yu, P. S., and Shu, K. Taxonomy-guided zero-shot recommendations with llms. *arXiv preprint arXiv:2406.14043*, 2024.
- Liu, C., He, S., Zhou, Q., Li, S., and Meng, W. Large language model guided knowledge distillation for time series anomaly detection. *arXiv preprint arXiv:2401.15123*, 2024a.
- Liu, H., Li, C., Wu, Q., and Lee, Y. J. Visual instruction tuning. *Advances in neural information processing systems*, 36, 2024b.
- Liu, J., Zhang, C., Qian, J., Ma, M., Qin, S., Bansal, C., Lin, Q., Rajmohan, S., and Zhang, D. Large language models can deliver accurate and interpretable time series anomaly detection. *arXiv preprint arXiv:2405.15370*, 2024c.
- Shukla, S. N. and Marlin, B. M. A survey on principles, models and methods for learning from irregularly sampled time series. *arXiv preprint arXiv:2012.00168*, 2020.
- Sui, Y., Zhou, M., Zhou, M., Han, S., and Zhang, D. Table meets llm: Can large language models understand structured table data? a benchmark and empirical study. In *Proceedings of the 17th ACM International Conference on Web Search and Data Mining*, pp. 645–654, 2024.
- Tabassum, A., Chinthavali, S., Tansakul, V., and Prakash, B. A. Actionable insights in urban multivariate time-series. In *Proceedings of the 30th ACM International Conference on Information & Knowledge Management*, pp. 1774–1783, 2021.
- Team, G., Georgiev, P., Lei, V. I., Burnell, R., Bai, L., Gulati, A., Tanzer, G., Vincent, D., Pan, Z., Wang, S., et al. Gemini 1.5: Unlocking multimodal understanding across millions of tokens of context. *arXiv preprint arXiv:2403.05530*, 2024.
- Wang, H., Rangapur, A., Xu, X., Liang, Y., Gharwi, H., Yang, C., and Shu, K. Piecing it all together: Verifying multi-hop multimodal claims. *arXiv preprint arXiv:2411.09547*, 2024a.
- Wang, P., Bai, S., Tan, S., Wang, S., Fan, Z., Bai, J., Chen, K., Liu, X., Wang, J., Ge, W., et al. Qwen2-vl: Enhancing vision-language model’s perception of the world at any resolution. *arXiv preprint arXiv:2409.12191*, 2024b.
- Wu, X., Huang, S., and Wei, F. Multimodal large language model is a human-aligned annotator for text-to-image generation. *arXiv preprint arXiv:2404.15100*, 2024.
- Xu, X., A. Brown, K., Mallick, T., Wang, X., Cruz-Camacho, E., B. Ross, R., D. Carothers, C., Lan, Z., and Shu, K. Surrogate modeling for hpc application iteration times forecasting with network features. In *Proceedings of the 38th ACM SIGSIM Conference on Principles of Advanced Discrete Simulation*, pp. 93–97, 2024a.
- Xu, X., Chen, C., Liang, Y., Huang, B., Bai, G., Zhao, L., and Shu, K. Sst: Multi-scale hybrid mamba-transformer experts for long-short range time series forecasting. *arXiv preprint arXiv:2404.14757*, 2024b.
- Yang, L., Wang, Y., Fan, X., Cohen, I., Chen, J., Zhao, Y., and Zhang, Z. Vitime: A visual intelligence-based foundation model for time series forecasting. *arXiv preprint arXiv:2407.07311*, 2024a.

- Yang, T., Nian, Y., Li, S., Xu, R., Li, Y., Li, J., Xiao, Z., Hu, X., Rossi, R., Ding, K., et al. Ad-llm: Benchmarking large language models for anomaly detection. *arXiv preprint arXiv:2412.11142*, 2024b.
- Yin, S., Fu, C., Zhao, S., Li, K., Sun, X., Xu, T., and Chen, E. A survey on multimodal large language models. *arXiv preprint arXiv:2306.13549*, 2023.
- Zamanzadeh Darban, Z., Webb, G. I., Pan, S., Aggarwal, C., and Salehi, M. Deep learning for time series anomaly detection: A survey. *ACM Computing Surveys*, 57(1): 1–42, 2024.
- Zhang, D., Li, S., Zhang, X., Zhan, J., Wang, P., Zhou, Y., and Qiu, X. Speechgpt: Empowering large language models with intrinsic cross-modal conversational abilities. *arXiv preprint arXiv:2305.11000*, 2023.
- Zhou, Z. and Yu, R. Can llms understand time series anomalies? *arXiv preprint arXiv:2410.05440*, 2024.
- Zhu, X., Xiong, Y., Wu, M., Nie, G., Zhang, B., and Yang, Z. Weather2k: A multivariate spatio-temporal benchmark dataset for meteorological forecasting based on real-time observation data from ground weather stations. *arXiv preprint arXiv:2302.10493*, 2023.
- Zhuang, J., Yan, L., Zhang, Z., Wang, R., Zhang, J., and Gu, Y. See it, think it, sorted: Large multimodal models are few-shot time series anomaly analyzers. *arXiv preprint arXiv:2411.02465*, 2024.

Appendix

A The Details of Multimodel LLMs

B Prompt Examples

C Hallucination Examples

D Time Series Image Examples

E Complete Results

A. The Details of Multimodal LLMs

GPT-4o (Achiam et al., 2023) is a state-of-the-art multimodal model released by OpenAI. It is designed to handle both text and vision tasks with high efficiency, and optimized for complex reasoning tasks, achieving notable performance on benchmarks such as MGSM (math reasoning) and HumanEval (coding). Its architecture, while not publicly disclosed, is engineered to maintain consistent performance across modalities, ensuring that the inclusion of images does not degrade text-based reasoning capabilities.

GPT-4o-mini (Achiam et al., 2023) is a streamlined, cost-efficient variant of GPT-4o, designed to replace GPT-3.5 while surpassing its performance. It demonstrates strong capabilities in mathematical reasoning and coding. The model is not open-sourced and supports both text and vision inputs via its API.

Gemini-1.5-Pro (Team et al., 2024) is a high-performance model designed for advanced reasoning and multimodal tasks built by Google. It supports a large context window and excels in tasks requiring deep understanding, such as mathematical reasoning and code generation. Its architecture, while not publicly disclosed, ensures robust performance across text and vision inputs, maintaining consistency even when processing multimodal queries.

Gemini-1.5-Flash (Team et al., 2024) is a lightweight, high-speed variant of the Gemini-1.5 series, tailored for applications requiring rapid inference and low latency. Despite its compact design, it delivers competitive performance on benchmarks like MGSM and HumanEval. The model supports multimodal inputs, including text and vision, and can be called by API.

LLaVA-NeXT-72B (Li et al., 2024a) is an advanced vision-language model tailored for high-performance multimodal understanding. It is open-source and built on a Qwen1.5-72B parameters architecture. It can integrate language and visual comprehension seamlessly, making it highly effective for image captioning, visual reasoning, and complex multimodal interactions. The model is designed to deliver state-of-the-art accuracy in vision-language tasks, with optimizations for both zero-shot and fine-tuned applications.

LLaVA-NeXT-8B (Li et al., 2024a) is a smaller, more efficient version of the LLaVA-NeXT series, designed for applications where computational resources are limited. Built on LLaMA3-8B parameters, it maintains strong performance on vision-language tasks, achieving competitive results on benchmarks like MMMU and VQA. The model is particularly well-suited for real-time applications requiring fast inference and low memory usage.

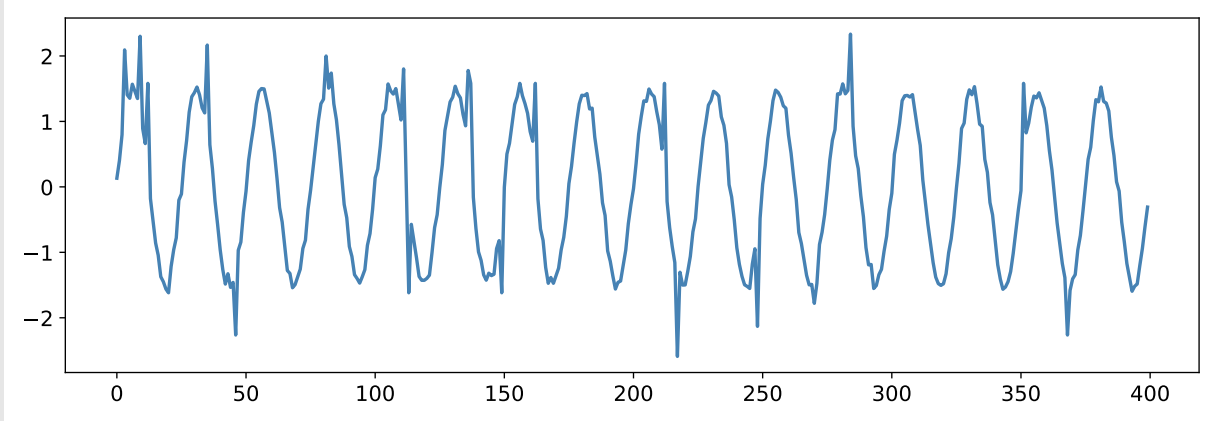
Qwen2-VL-72B-Instruct (Wang et al., 2024b) is a large multimodal model optimized for instruction-following tasks involving both text and vision developed by Alibaba. With 72B parameters, it delivers robust performance on benchmarks such as MMMU and VQA. The model is designed to handle complex queries that require deep reasoning across modalities, ensuring consistent performance even when processing multimodal inputs. Its architecture is tailored for applications requiring high accuracy and reliability.

Qwen2-VL-7B-Instruct (Wang et al., 2024b) is a compact version of the Qwen2-VL series, designed for scenarios where computational efficiency is paramount. Despite its smaller size, it achieves competitive results on vision-language benchmarks, making it suitable for real-time applications. The model is optimized for instruction-following tasks, ensuring that it can handle multimodal inputs without compromising performance.

B. Prompt Examples

Prompt for Point-Wise Time Series Anomalies

Input Image:

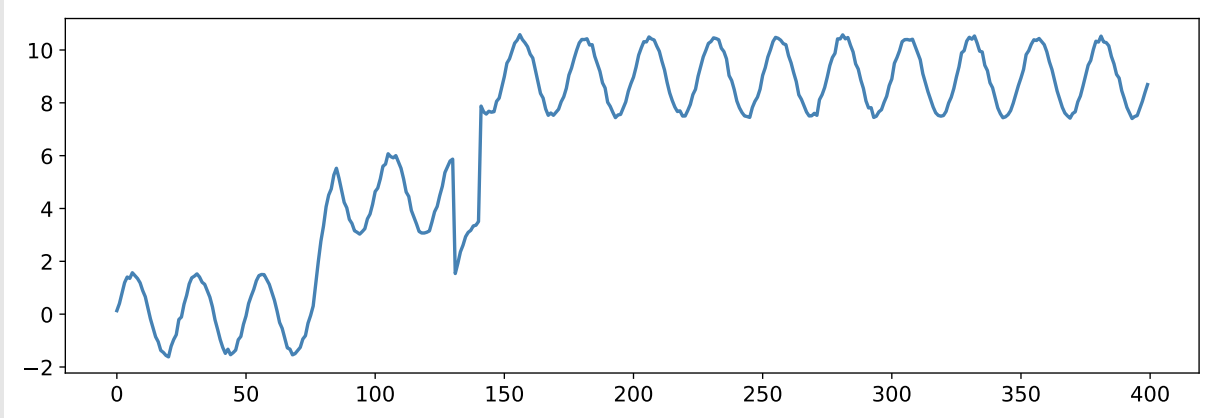


Prompt: Detect points of anomalies in this time series, in terms of the x-axis coordinate. List one by one in a list. For example, if points $x=2, 51,$ and 106 are anomalies, then output "[2, 51, 106]". If there are no anomalies, answer with an empty list [].

Response: [3, 9, 12, 35, 46, 81, 83, 111, 113, 136, 137, 149, 162, 212, 217, 248, 270, 284, 351, 368]

Prompt for Range-Wise Time Series Anomalies

Input Image:

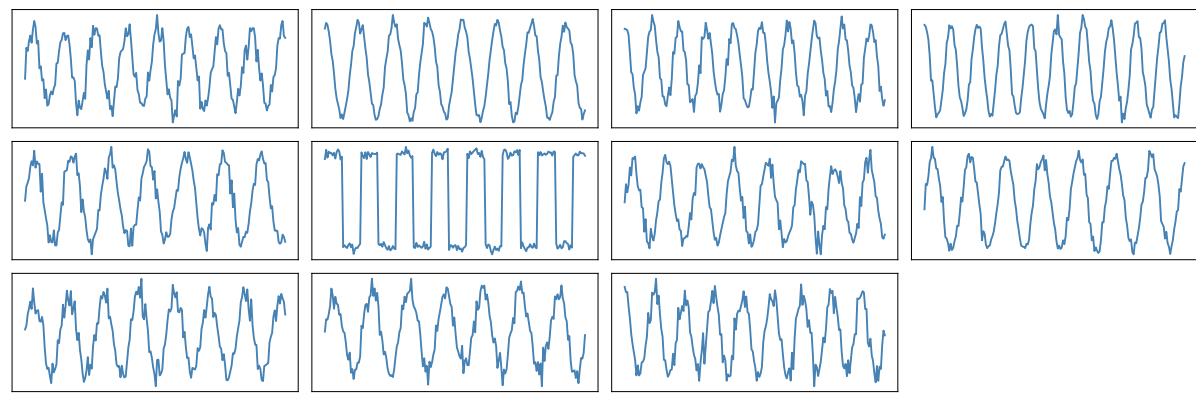


Prompt: Detect ranges of anomalies in this time series, in terms of the x-axis coordinate. List one by one in a list. For example, if ranges (including two endpoints) [2, 11], [50, 60], and [105, 118], are anomalies, then output "[[2, 11], [50, 60], [105, 118]]". If there are no anomalies, answer with an empty list [].

Response: [[76, 85], [131, 140]]

Prompt for Variate-Wise Time Series Anomalies

Input Image:



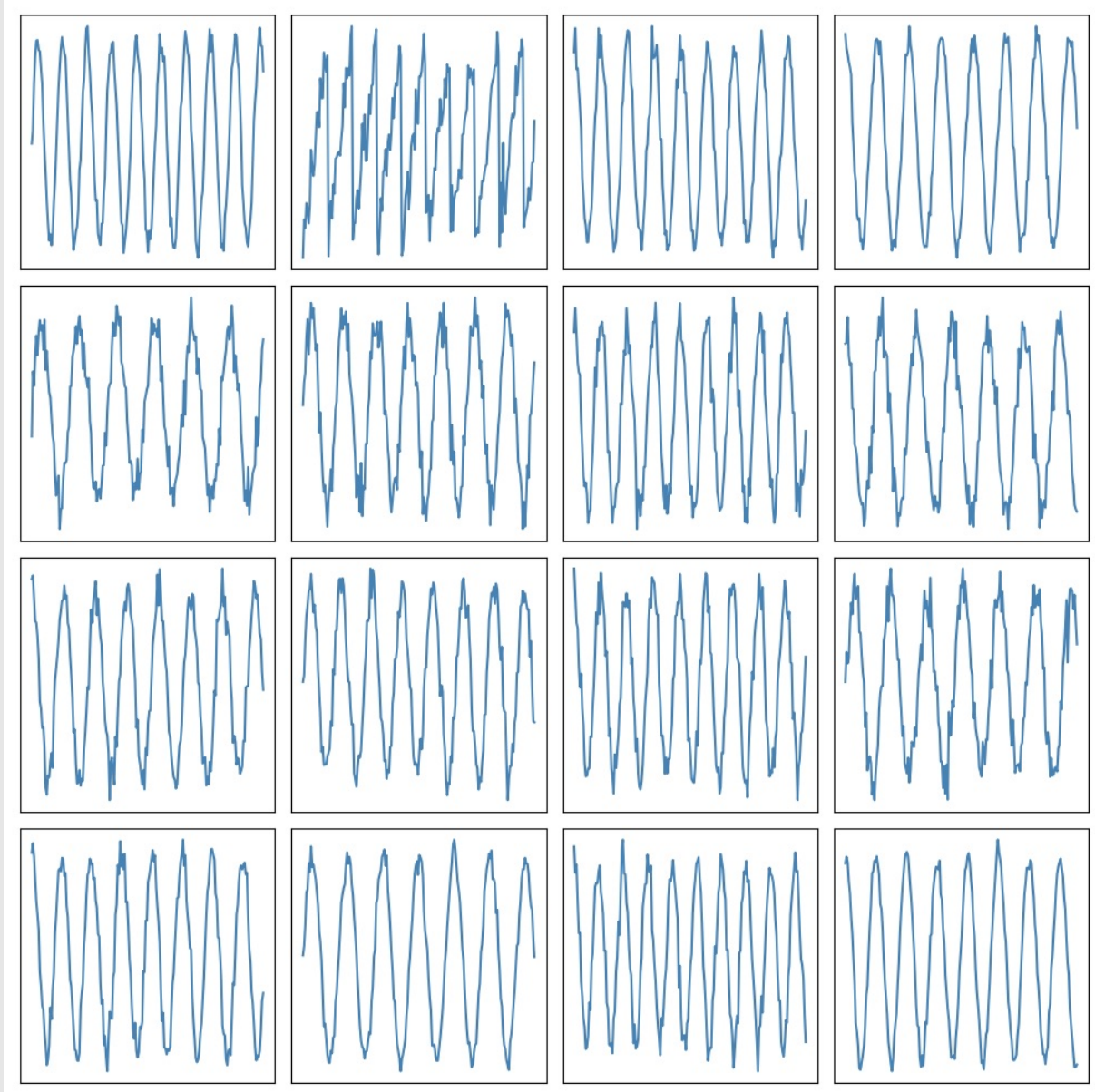
Prompt: Detect univariate time series of anomalies in this multivariate time series, in terms of ID of univariate time series. The image is a multivariate time series including multiple subimages to indicate multiple univariate time series. From left to right and top to bottom, the ID of each subimage increases by 1, starting from 0. List one by one in a list. For example, if ID=0, 2, and 5 are anomalous univariate time series, then output "[0, 2, 5]". If there are no anomalies, answer with an empty list [].

Response: [5]

C. Hallucination Examples

Hallucination of LLaVA-NeXT-8B for 16-Variates Time Series Anomalies Detection (Sawtooth)

Input Image:

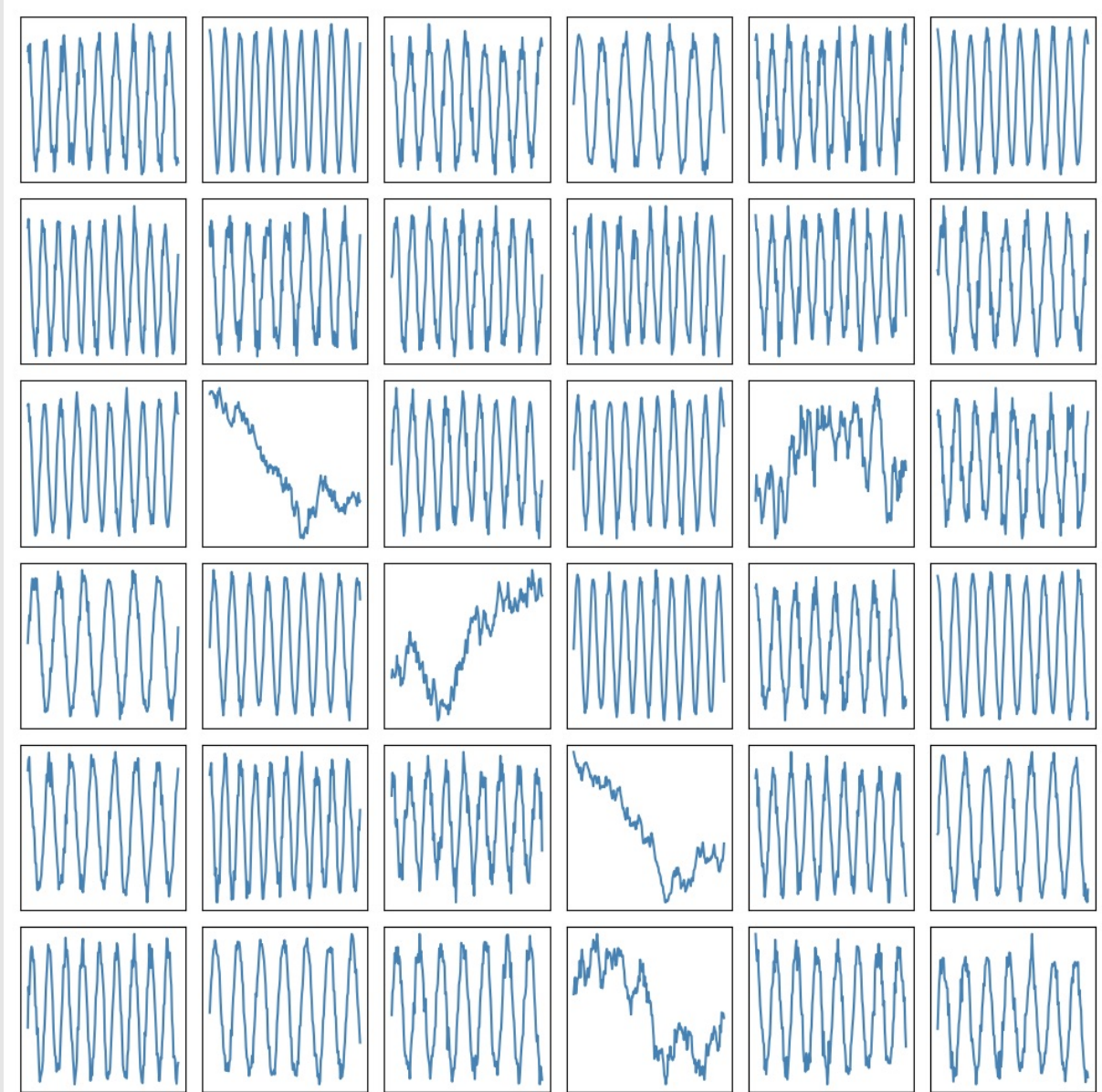


Prompt: Detect univariate time series of anomalies in this multivariate time series, in terms of ID of univariate time series. The image is a multivariate time series including multiple subimages to indicate multiple univariate time series. From left to right and top to bottom, the ID of each subimage increases by 1, starting from 0. List one by one in a list. For example, if ID=0, 2, and 5 are anomalous univariate time series, then output "[0, 2, 5]". If there are no anomalies, answer with an empty list [].

LLaVA-NeXT-8B Response: [0, 2, 5, 8, 11, 14, 17, 20, 23, 26, 29, 32, 35, 38, 41, 44, 47, 50, 53, 56, 59, 62, 65, 68, 71, 74, 77, 80, 83, 86, 89, 92, 95, 98, 101, ..., 999]

Hallucination of LLaVA-NeXT-8B for 36-Variates Time Series Anomalies Detection (Random)

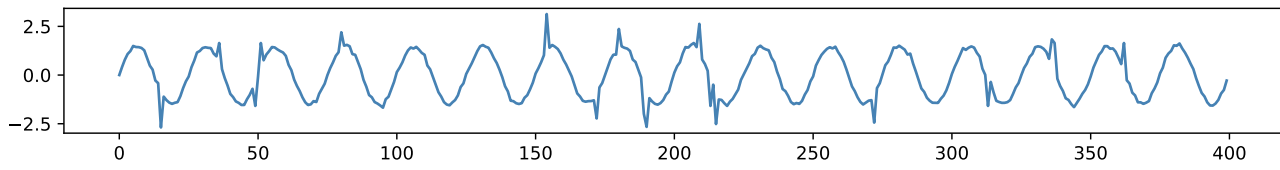
Input Image:



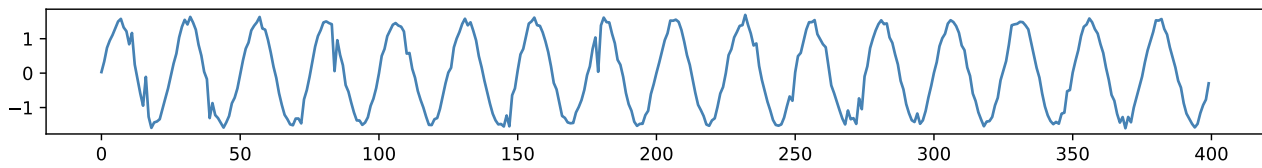
Prompt: Detect univariate time series of anomalies in this multivariate time series, in terms of ID of univariate time series. The image is a multivariate time series including multiple subimages to indicate multiple univariate time series. From left to right and top to bottom, the ID of each subimage increases by 1, starting from 0. List one by one in a list. For example, if ID=0, 2, and 5 are anomalous univariate time series, then output "[0, 2, 5]". If there are no anomalies, answer with an empty list [].

LLaVA-NeXT-8B Response: [0, 1, 2, 3, 4, 5, 6, 7, 8, 9, 10, 11, 12, 13, 14, 15, 16, 17, 18, 19, 20, 21, 22, 23, 24, 25, 26, 27, 28, 29, 30, 31, 32, 33, 34, 35, 36, 37, 38, 39, 40, 41, 42, 43, 44, 45, 46, 47, 48, 49, 50, ..., 995, 996, 997]

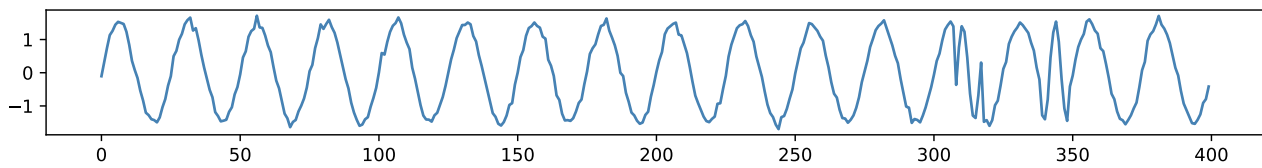
D. Time Series Image Examples



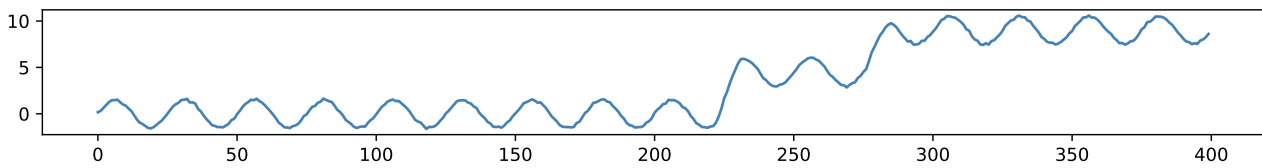
(a) Global



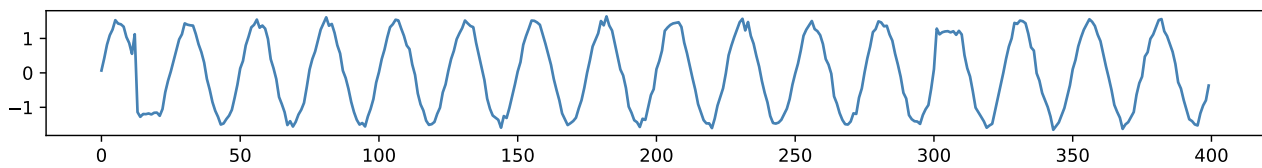
(b) Contextual



(c) Seasonal

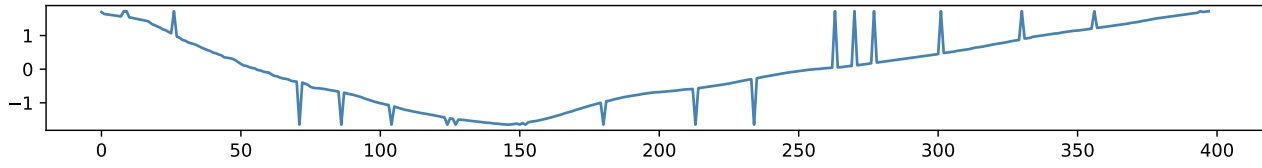


(d) Trend

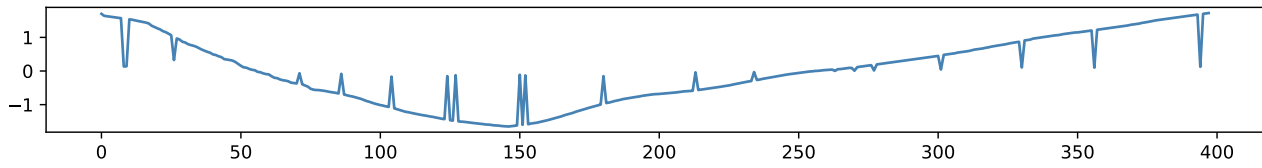


(e) Shapelet

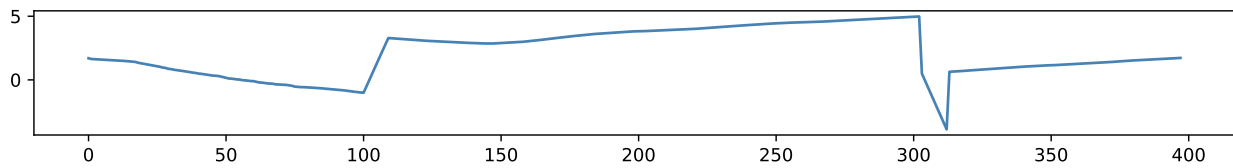
Figure 6: Univariate TSI (Sine)



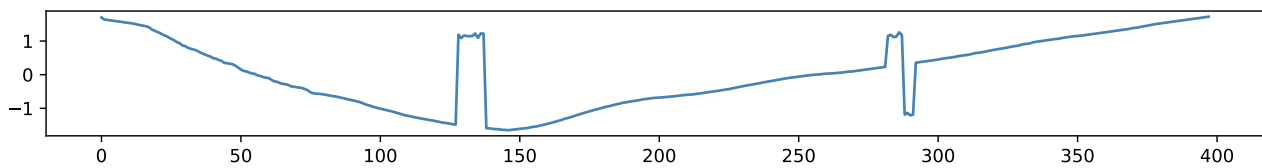
(a) Global



(b) Contextual



(c) Trend



(d) Shapelet

Figure 7: Univariate TSI (Symbols)

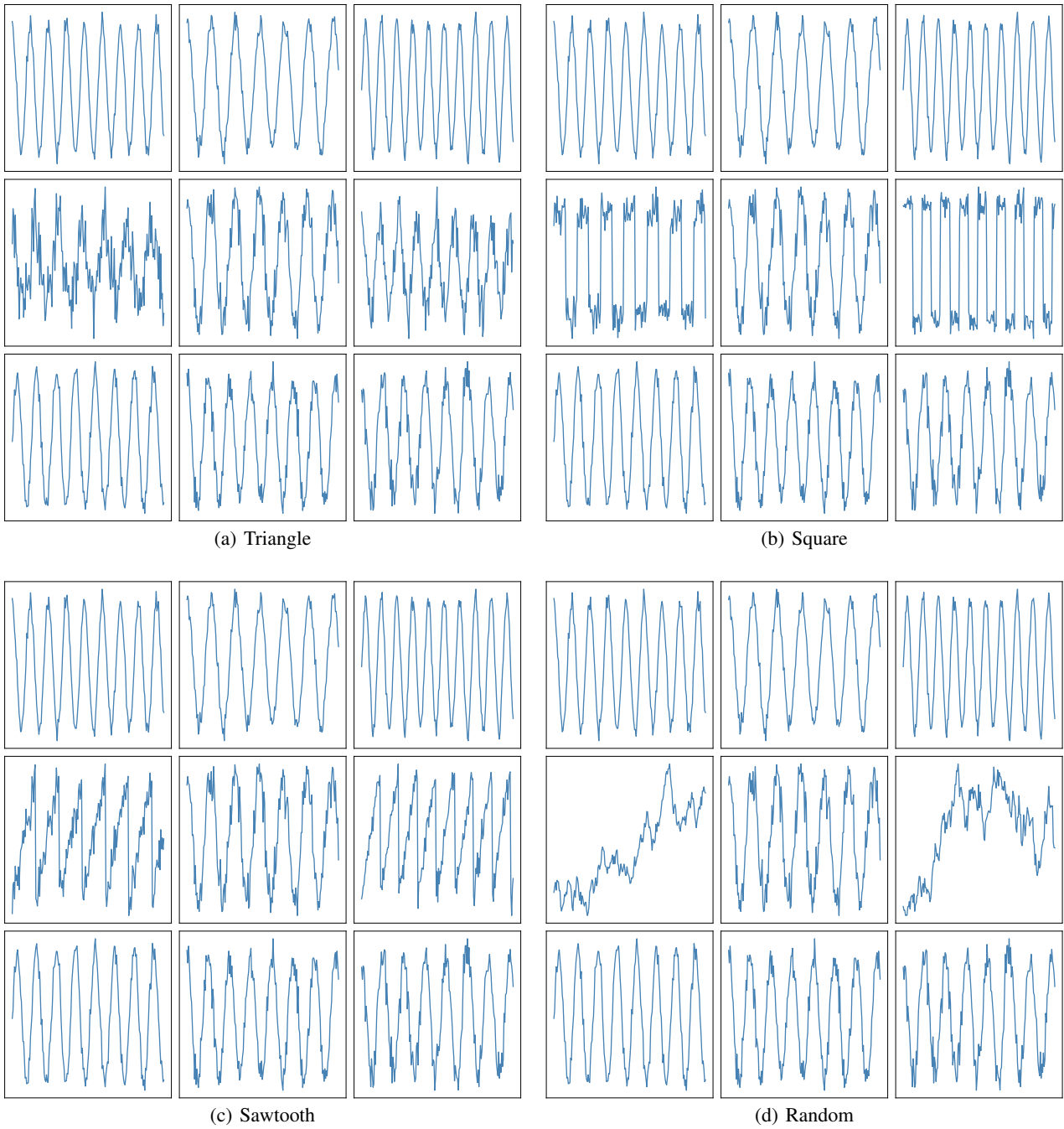


Figure 8: Multivariate TSI (Sine/Cosine)

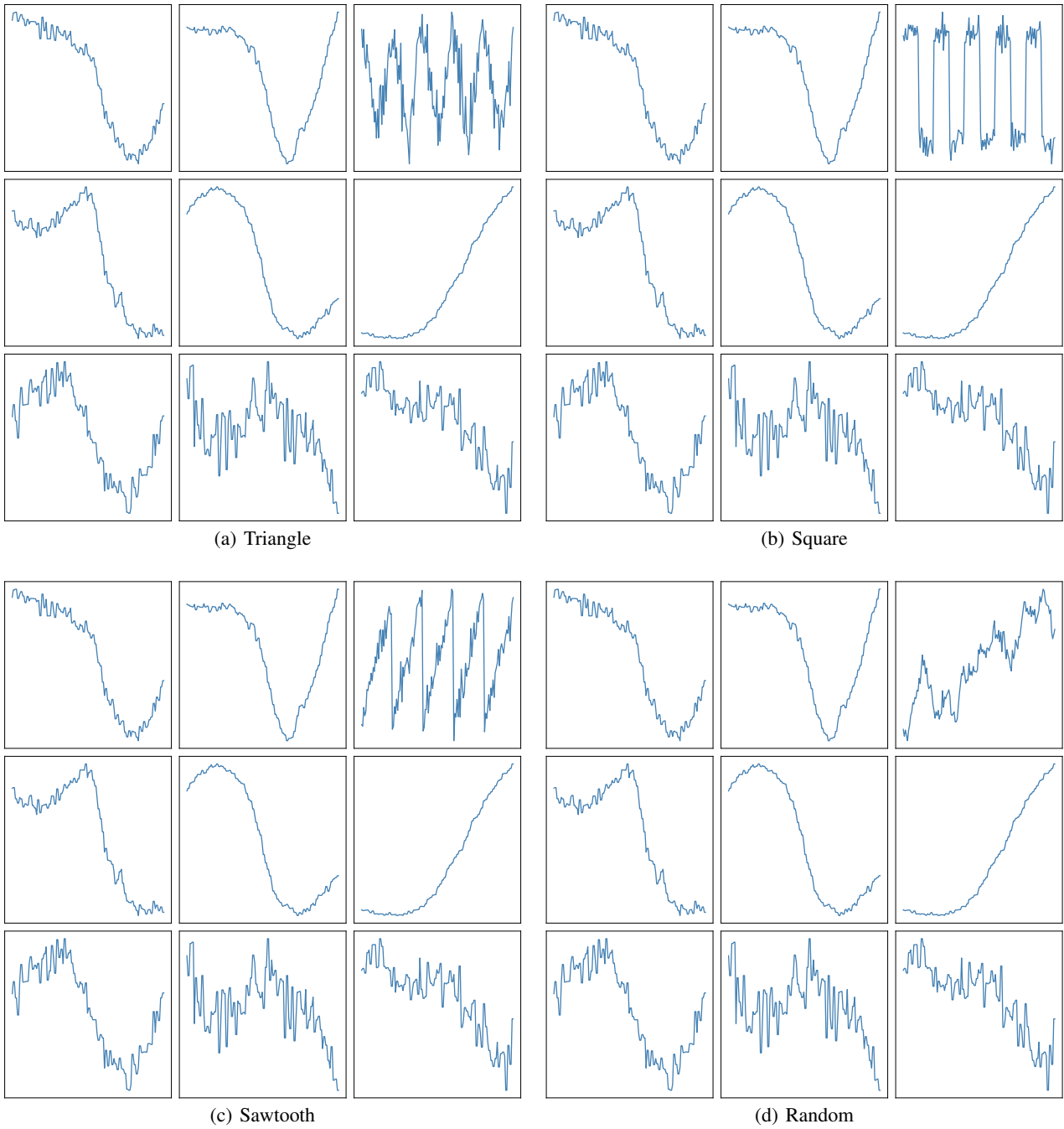


Figure 9: Multivariate TSI (ArticulatoryWordRecognition)

Can Multimodal LLMs Perform Time Series Anomaly Detection?

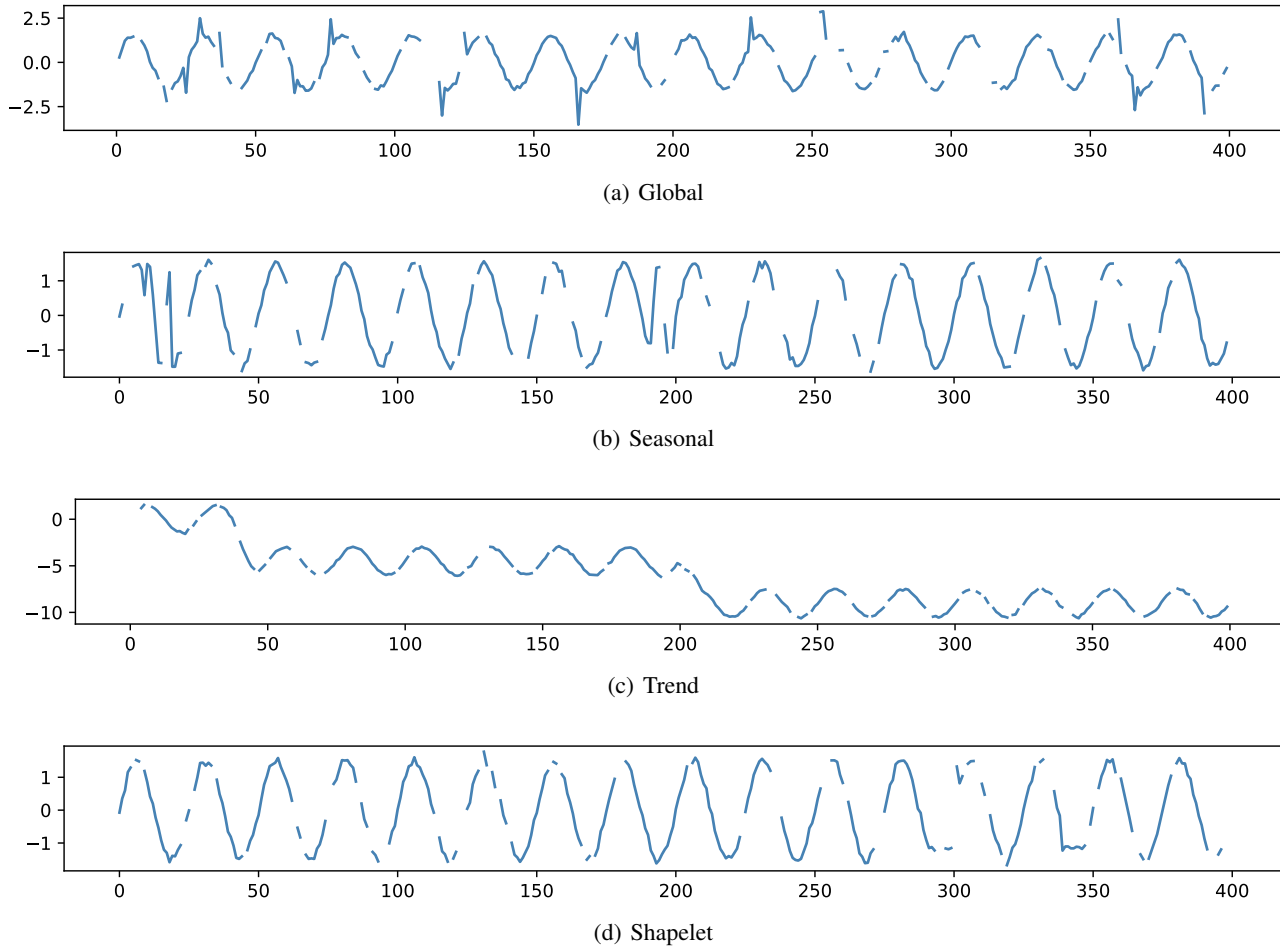


Figure 10: Irregular Univariate TSI (Sine, $r = 15\%$)

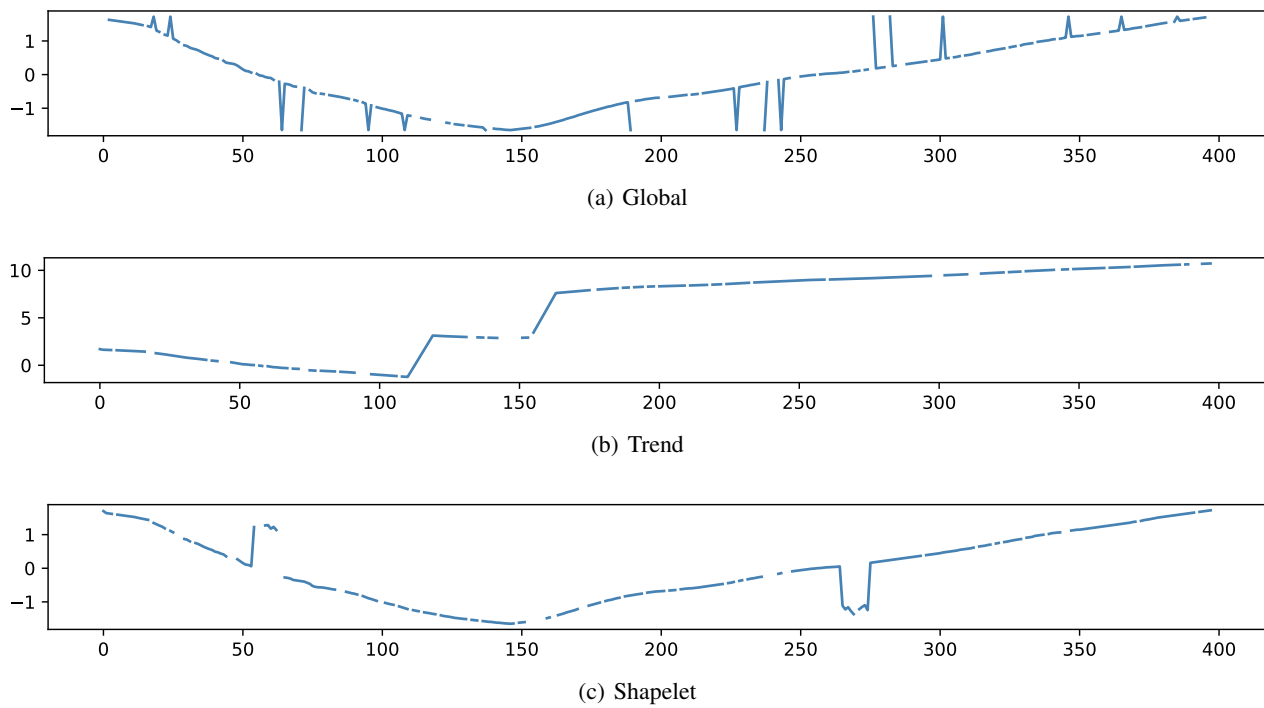


Figure 11: Irregular Univariate TSI (Symbols, $r = 15\%$)

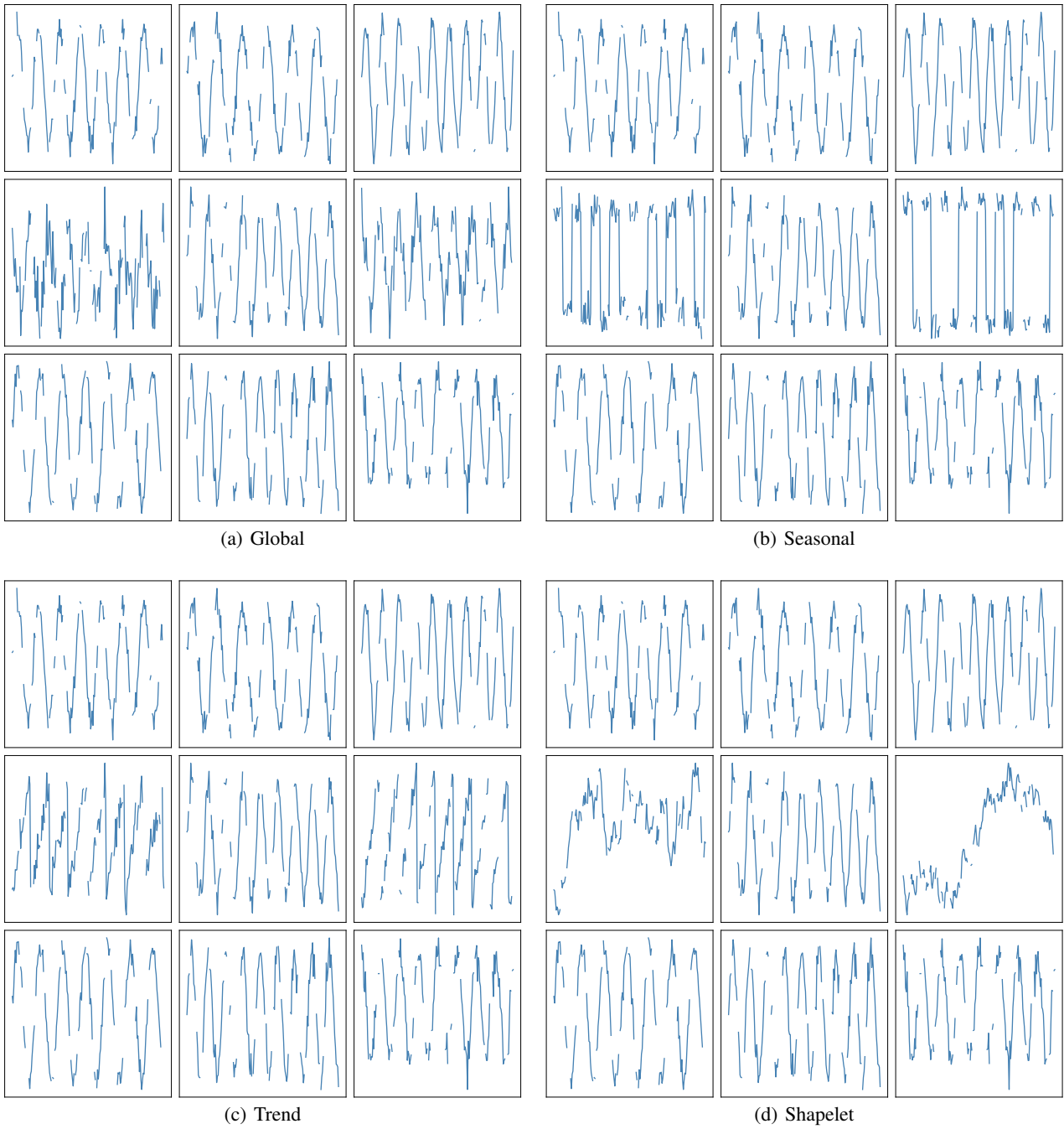


Figure 12: Irregular Multivariate TSI (ArticulatoryWordRecognition, $r = 15\%$)

E. Complete Results

Table 5: Performance of MLLMs on multivariate time series anomalies ($M = 4$)

Anomaly Metrics	Triangle			Square			Sawtooth			Random		
	P	R	F1	P	R	F1	P	R	F1	P	R	F1
GPT-4o	<u>60.71</u>	<u>79.76</u>	<u>66.48</u>	<u>85.68</u>	100.00	<u>90.18</u>	76.50	<u>91.57</u>	81.33	89.15	100.00	92.64
GPT-4o-mini	8.92	17.00	11.40	38.58	73.00	49.05	13.25	29.00	17.74	39.83	60.00	46.01
Gemini-1.5-Pro	67.50	81.00	71.84	97.50	100.00	98.34	93.50	99.00	95.34	100.00	100.00	100.00
Gemini-1.5-Flash	51.33	61.00	54.51	73.83	<u>81.00</u>	76.17	<u>82.50</u>	91.00	<u>85.34</u>	<u>98.50</u>	<u>99.00</u>	<u>98.67</u>
LLaVA-NeXT-72B	27.46	78.57	39.43	23.71	71.13	34.65	23.89	75.51	35.65	24.83	63.00	33.94
LLaVA-NeXT-8B	22.50	45.00	30.02	22.50	45.00	30.02	22.50	45.00	30.02	22.50	45.00	30.02
Qwen2-VL-72B-Instruct	46.00	62.00	50.97	44.25	63.00	50.08	55.67	68.00	59.30	70.33	74.00	71.30
Qwen2-VL-7B-Instruct	29.50	43.00	33.20	37.08	56.00	42.44	36.75	56.00	42.07	46.75	64.00	51.20

Table 6: Performance of MLLMs on multivariate time series anomalies ($M = 9$)

Anomaly Metrics	Triangle			Square			Sawtooth			Random		
	P	R	F1									
GPT-4o	<u>39.59</u>	76.06	<u>47.12</u>	56.88	<u>82.41</u>	63.28	43.02	86.49	53.58	<u>84.52</u>	<u>92.86</u>	<u>86.79</u>
GPT-4o-mini	8.46	23.00	11.82	20.68	48.50	27.82	8.13	20.50	11.26	32.92	60.00	40.79
Gemini-1.5-Pro	53.05	56.50	51.15	81.42	87.00	82.52	80.25	<u>84.50</u>	80.47	92.07	93.50	92.54
Gemini-1.5-Flash	37.57	50.50	39.21	<u>70.58</u>	76.50	<u>70.70</u>	<u>62.67</u>	68.00	<u>61.94</u>	81.67	80.00	79.94
LLaVA-NeXT-72B	15.24	<u>59.38</u>	23.20	16.38	65.82	24.66	14.06	58.85	21.36	18.66	55.56	25.27
LLaVA-NeXT-8B	15.25	44.50	22.19	15.25	44.50	22.19	15.25	44.50	22.19	15.08	45.50	21.99
Qwen2-VL-72B-Instruct	32.57	52.00	37.49	29.48	51.00	35.57	36.73	52.50	40.67	64.83	70.50	66.27
Qwen2-VL-7B-Instruct	21.79	29.50	22.32	26.87	41.00	29.00	20.04	29.00	21.68	39.69	45.00	39.22

Table 7: Performance of MLLMs on multivariate time series anomalies ($M = 16$)

Anomaly Metrics	Triangle			Square			Sawtooth			Random		
	P	R	F1									
GPT-4o	26.58	64.22	<u>31.95</u>	37.84	<u>69.89</u>	45.55	23.24	69.91	32.53	59.62	<u>61.99</u>	60.05
GPT-4o-mini	8.98	24.00	12.23	12.59	32.50	17.13	3.71	9.66	4.95	29.04	42.50	32.42
Gemini-1.5-Pro	45.61	43.00	40.12	73.34	78.00	74.41	61.53	<u>69.17</u>	62.10	84.34	84.84	84.37
Gemini-1.5-Flash	<u>33.41</u>	34.16	30.59	<u>57.33</u>	56.00	<u>54.25</u>	<u>44.00</u>	45.50	<u>41.50</u>	<u>60.57</u>	61.67	<u>60.42</u>
LLaVA-NeXT-72B	11.62	<u>57.65</u>	17.35	12.87	63.37	19.42	12.44	61.40	18.34	12.32	44.10	17.02
LLaVA-NeXT-8B	13.01	40.66	19.01	13.20	41.66	19.33	13.20	41.66	19.33	13.11	51.50	19.61
Qwen2-VL-72B-Instruct	20.46	32.50	23.03	17.29	34.00	21.07	18.52	32.83	22.05	35.55	36.50	34.72
Qwen2-VL-7B-Instruct	11.25	19.50	10.64	21.52	38.83	21.80	10.85	21.17	11.44	30.66	33.50	27.72

Table 8: Performance of MLLMs on multivariate time series anomalies ($M = 25$)

Anomaly Metrics	Triangle			Square			Sawtooth			Random		
	P	R	F1									
GPT-4o	19.11	<u>42.26</u>	<u>22.90</u>	23.01	43.13	<u>28.41</u>	15.77	<u>47.72</u>	<u>21.35</u>	<u>39.60</u>	42.22	<u>40.67</u>
GPT-4o-mini	4.03	8.08	4.97	2.93	8.17	4.18	0.00	0.00	0.00	12.53	14.91	13.33
Gemini-1.5-Pro	31.62	30.50	27.97	50.93	<u>51.67</u>	50.27	41.48	45.42	41.32	65.37	62.75	63.76
Gemini-1.5-Flash	<u>24.18</u>	18.75	18.67	<u>32.40</u>	28.16	28.25	<u>20.81</u>	18.42	18.23	33.25	31.41	31.95
LLaVA-NeXT-72B	9.98	53.69	13.32	9.30	59.29	14.17	9.84	58.97	14.89	8.85	44.19	13.25
LLaVA-NeXT-8B	9.15	35.75	14.10	9.49	38.16	14.62	9.32	35.50	14.28	9.25	<u>44.42</u>	14.56
Qwen2-VL-72B-Instruct	13.27	25.00	15.85	13.23	29.74	16.50	11.89	28.49	15.12	18.19	18.08	17.72
Qwen2-VL-7B-Instruct	11.81	15.58	9.38	9.39	25.08	10.07	3.72	9.00	3.68	17.18	25.33	14.99

Table 9: Performance of MLLMs on multivariate time series anomalies ($M = 36$)

Anomaly Metrics	Triangle			Square			Sawtooth			Random		
	P	R	F1									
GPT-4o	<u>12.12</u>	26.08	<u>14.61</u>	14.32	29.34	17.78	9.07	27.82	12.59	23.90	25.79	<u>24.60</u>
GPT-4o-mini	2.86	5.02	3.42	0.61	2.00	0.92	0.39	1.45	0.60	7.73	9.35	8.27
Gemini-1.5-Pro	18.72	17.38	15.84	30.73	31.66	30.39	25.53	25.12	24.00	34.21	32.56	33.25
Gemini-1.5-Flash	11.52	10.03	9.71	<u>26.10</u>	19.71	<u>21.51</u>	<u>16.98</u>	12.53	<u>13.43</u>	<u>25.86</u>	22.90	24.00
LLaVA-NeXT-72B	6.11	46.72	9.61	8.18	54.40	11.97	9.34	56.26	13.21	8.53	<u>38.17</u>	11.19
LLaVA-NeXT-8B	7.42	<u>43.50</u>	12.04	8.91	<u>52.27</u>	14.47	8.33	<u>48.00</u>	13.00	7.96	51.97	13.09
Qwen2-VL-72B-Instruct	8.00	19.63	9.79	7.91	25.18	10.64	6.57	22.00	8.99	16.70	17.41	14.28
Qwen2-VL-7B-Instruct	11.47	7.48	7.21	10.17	15.81	7.33	5.61	3.25	3.34	17.86	23.23	13.49

Table 10: Performance of MLLMs on irregular univariate time series anomalies ($r = 5\%$)

Anomaly Metrics	Irr-Global			Irr-Seasonal			Irr-Trend			Irr-Shaplet		
	P	R	F1									
GPT-4o	49.13	11.66	15.97	49.47	51.17	48.22	79.98	73.87	<u>74.26</u>	<u>61.86</u>	65.86	<u>61.92</u>
GPT-4o-mini	43.61	14.11	<u>20.58</u>	18.13	27.84	21.57	61.74	68.65	<u>62.57</u>	<u>51.85</u>	78.48	61.67
Gemini-1.5-Pro	63.02	10.56	17.17	<u>45.21</u>	42.50	42.06	79.12	72.21	72.71	62.12	<u>68.93</u>	63.26
Gemini-1.5-Flash	<u>57.99</u>	8.11	13.78	26.24	25.60	24.90	90.38	78.51	81.60	55.72	63.54	57.93
LLaVA-NeXT-72B	47.52	8.82	14.43	39.27	48.51	42.09	57.99	62.01	58.28	49.74	54.69	50.41
LLaVA-NeXT-8B	49.36	<u>13.87</u>	21.17	20.11	32.56	24.69	27.82	46.41	34.37	21.70	36.54	26.99
Qwen2-VL-72B-Instruct	54.35	11.38	17.77	19.64	21.61	20.06	<u>80.07</u>	<u>74.15</u>	74.10	57.23	58.29	56.59
Qwen2-VL-7B-Instruct	47.67	7.65	13.04	43.20	<u>49.24</u>	<u>45.03</u>	56.28	61.01	56.45	52.00	65.77	56.77

Table 11: Performance of MLLMs on irregular univariate time series anomalies ($r = 10\%$)

Anomaly Metrics	Irr-Global			Irr-Seasonal			Irr-Trend			Irr-Shaplet		
	P	R	F1									
GPT-4o	48.48	16.04	19.51	46.55	49.84	46.53	<u>82.64</u>	<u>74.16</u>	<u>75.49</u>	61.40	<u>75.01</u>	66.02
GPT-4o-mini	49.94	<u>15.89</u>	23.49	16.99	27.96	20.87	67.01	72.78	66.56	51.54	81.00	<u>62.43</u>
Gemini-1.5-Pro	59.13	9.66	15.85	<u>46.01</u>	40.11	41.24	81.54	70.06	72.36	<u>59.16</u>	66.96	60.17
Gemini-1.5-Flash	56.03	6.95	12.01	24.72	23.76	22.64	88.24	76.77	79.79	49.68	62.03	53.64
LLaVA-NeXT-72B	50.13	9.88	16.08	45.25	54.79	47.72	59.42	59.34	57.47	54.15	59.84	55.45
LLaVA-NeXT-8B	46.62	14.40	<u>21.55</u>	18.47	31.61	22.99	21.28	32.76	24.75	24.56	44.17	31.25
Qwen2-VL-72B-Instruct	<u>57.53</u>	14.04	19.85	16.57	17.78	16.35	78.40	71.99	72.16	47.17	47.74	46.53
Qwen2-VL-7B-Instruct	47.16	7.88	13.27	45.68	<u>51.22</u>	<u>47.25</u>	54.31	59.16	55.05	51.97	70.10	58.31

Table 12: Performance of MLLMs on irregular univariate time series anomalies ($r = 15\%$)

Anomaly Metrics	Irr-Global			Irr-Seasonal			Irr-Trend			Irr-Shaplet		
	P	R	F1									
GPT-4o	45.55	16.96	19.43	41.26	49.21	43.44	78.41	71.80	72.26	<u>59.73</u>	<u>74.94</u>	65.04
GPT-4o-mini	48.71	<u>15.55</u>	22.95	24.85	42.48	31.09	64.12	71.08	64.52	50.80	81.60	<u>62.11</u>
Gemini-1.5-Pro	60.04	10.14	16.50	<u>43.79</u>	39.61	39.74	<u>80.41</u>	71.10	<u>72.48</u>	63.03	65.52	61.06
Gemini-1.5-Flash	44.84	5.39	9.39	26.46	31.04	26.64	86.43	78.76	80.23	32.72	49.16	38.52
LLaVA-NeXT-72B	48.32	9.97	15.94	43.40	54.16	<u>46.82</u>	62.53	64.22	61.38	48.24	61.12	52.59
LLaVA-NeXT-8B	49.74	14.50	<u>21.79</u>	13.56	24.13	17.19	22.36	33.87	26.29	33.72	58.28	42.14
Qwen2-VL-72B-Instruct	<u>56.72</u>	13.22	18.73	9.94	10.84	9.81	76.12	<u>73.90</u>	72.07	30.66	29.90	29.55
Qwen2-VL-7B-Instruct	47.30	7.81	13.19	47.85	<u>52.83</u>	49.04	52.37	57.47	53.34	48.67	68.15	55.36

Table 13: Performance of MLLMs on irregular univariate time series anomalies ($r = 20\%$)

Anomaly Metrics	Irr-Global			Irr-Seasonal			Irr-Trend			Irr-Shaplet		
	P	R	F1									
GPT-4o	50.07	<u>15.60</u>	19.11	47.18	<u>54.40</u>	48.53	78.39	70.90	<u>71.85</u>	58.63	<u>75.69</u>	64.33
GPT-4o-mini	49.92	16.05	23.71	31.19	50.55	38.14	62.60	73.36	64.88	49.26	83.35	<u>61.55</u>
Gemini-1.5-Pro	60.90	9.07	15.11	43.13	37.82	38.43	<u>79.74</u>	69.41	71.26	<u>51.47</u>	50.63	48.15
Gemini-1.5-Flash	43.13	5.95	10.18	23.50	35.48	27.12	86.90	76.13	78.66	26.38	44.76	32.48
LLaVA-NeXT-72B	49.51	10.81	17.14	48.92	59.00	52.01	55.75	61.34	56.91	45.15	56.50	48.80
LLaVA-NeXT-8B	47.95	14.00	<u>20.86</u>	16.77	28.20	20.74	27.08	45.35	33.61	34.65	62.16	43.96
Qwen2-VL-72B-Instruct	<u>56.91</u>	12.26	18.30	9.33	10.16	9.23	74.69	<u>73.51</u>	71.54	20.79	20.23	20.01
Qwen2-VL-7B-Instruct	48.26	7.98	13.44	<u>48.34</u>	53.08	<u>49.47</u>	52.23	57.67	53.38	50.92	71.95	58.17

Table 14: Performance of MLLMs on irregular univariate time series anomalies ($r = 25\%$)

Anomaly Metrics	Irr-Global			Irr-Seasonal			Irr-Trend			Irr-Shaplet		
	P	R	F1									
GPT-4o	49.28	19.71	<u>22.30</u>	44.14	57.94	<u>48.48</u>	78.54	73.81	<u>73.59</u>	58.13	<u>73.98</u>	62.57
GPT-4o-mini	50.26	<u>16.96</u>	24.18	36.32	61.43	45.21	62.25	<u>74.22</u>	65.56	47.78	83.73	<u>60.60</u>
Gemini-1.5-Pro	60.01	9.41	15.71	41.47	38.83	38.39	<u>79.16</u>	69.22	70.99	46.30	39.16	40.29
Gemini-1.5-Flash	43.05	5.70	9.81	28.72	49.78	35.50	84.28	79.42	79.55	37.52	67.38	47.49
LLaVA-NeXT-72B	46.52	11.05	17.09	51.96	<u>60.21</u>	53.77	55.90	61.81	57.16	47.25	57.04	50.43
LLaVA-NeXT-8B	47.09	14.88	21.83	23.35	40.36	29.43	21.52	36.21	26.55	28.32	52.81	36.80
Qwen2-VL-72B-Instruct	<u>51.31</u>	11.94	16.98	13.23	12.31	12.34	73.13	71.09	69.54	22.68	22.26	22.16
Qwen2-VL-7B-Instruct	44.50	7.11	12.00	<u>47.00</u>	49.67	47.38	51.62	57.31	52.60	<u>47.79</u>	60.42	51.94

Table 15: Performance of MLLMs on irregular multivariate time series anomalies ($r = 5\%$)

Anomaly Metrics	Irr-Triangle			Irr-Square			Irr-Sawtooth			Irr-Random		
	P	R	F1									
GPT-4o	32.14	80.53	<u>42.25</u>	44.37	<u>78.72</u>	<u>52.96</u>	30.04	<u>76.63</u>	40.20	<u>88.26</u>	93.48	<u>89.68</u>
GPT-4o-mini	18.13	62.50	27.21	18.38	62.00	27.36	15.56	56.00	23.48	26.71	65.50	36.24
Gemini-1.5-Pro	55.08	53.50	51.61	82.17	85.00	82.87	79.50	86.00	80.74	91.00	<u>91.50</u>	91.17
Gemini-1.5-Flash	<u>36.07</u>	41.00	36.24	<u>50.99</u>	55.00	51.21	<u>50.00</u>	55.50	<u>50.44</u>	73.84	76.50	74.04
LLaVA-NeXT-72B	16.53	<u>70.00</u>	25.31	15.58	65.31	23.67	15.33	65.15	23.74	17.04	58.67	24.53
LLaVA-NeXT-8B	14.12	49.00	21.01	16.86	63.50	25.36	15.33	55.50	23.20	17.37	55.00	25.27
Qwen2-VL-72B-Instruct	28.55	45.00	33.20	21.66	40.50	27.27	25.83	41.00	30.17	55.00	57.00	55.50
Qwen2-VL-7B-Instruct	19.74	25.50	20.13	18.70	29.00	20.69	13.25	23.50	15.75	46.75	47.50	43.97

Table 16: Performance of MLLMs on irregular multivariate time series anomalies ($r = 10\%$)

Anomaly Metrics	Irr-Triangle			Irr-Square			Irr-Sawtooth			Irr-Random		
	P	R	F1									
GPT-4o	<u>35.16</u>	74.74	<u>43.07</u>	53.18	<u>81.25</u>	<u>60.39</u>	28.43	<u>74.24</u>	37.96	<u>88.95</u>	90.53	<u>89.40</u>
GPT-4o-mini	17.00	59.50	25.35	17.59	62.50	26.59	16.46	62.50	25.07	21.47	60.50	29.98
Gemini-1.5-Pro	49.58	46.00	46.14	83.83	83.50	83.30	75.63	75.00	73.84	90.33	<u>90.50</u>	90.27
Gemini-1.5-Flash	31.23	32.50	29.71	<u>53.90</u>	58.50	54.61	<u>39.92</u>	43.50	<u>39.74</u>	74.67	74.00	72.94
LLaVA-NeXT-72B	14.67	<u>64.06</u>	22.81	15.42	66.84	23.94	15.32	61.00	23.20	17.87	54.59	24.69
LLaVA-NeXT-8B	16.14	51.50	23.73	16.41	57.00	24.53	15.90	50.00	23.27	13.91	48.50	20.74
Qwen2-VL-72B-Instruct	21.91	35.50	25.94	24.66	43.50	30.14	20.33	32.50	23.90	44.83	51.00	46.47
Qwen2-VL-7B-Instruct	13.58	21.00	15.33	16.16	30.50	19.97	9.24	18.50	11.57	35.33	47.00	36.96

Table 17: Performance of MLLMs on irregular multivariate time series anomalies ($r = 15\%$)

Anomaly Metrics	Irr-Triangle			Irr-Square			Irr-Sawtooth			Irr-Random		
	P	R	F1									
GPT-4o	<u>28.69</u>	<u>61.98</u>	<u>35.19</u>	<u>70.49</u>	84.74	<u>74.05</u>	<u>28.22</u>	69.27	<u>37.09</u>	<u>88.45</u>	<u>88.64</u>	<u>88.37</u>
GPT-4o-mini	16.41	60.00	24.78	18.44	61.00	27.17	15.28	55.50	23.03	23.76	62.50	32.47
Gemini-1.5-Pro	53.53	48.00	48.41	81.00	<u>79.50</u>	79.73	56.54	55.50	54.37	90.50	89.50	89.83
Gemini-1.5-Flash	20.23	20.50	18.54	42.92	45.00	42.97	18.67	22.00	18.90	73.50	74.00	72.34
LLaVA-NeXT-72B	14.29	62.89	22.33	17.62	67.86	25.76	16.35	<u>63.78</u>	24.53	17.84	61.34	25.75
LLaVA-NeXT-8B	15.29	47.00	22.09	15.43	54.50	23.14	16.43	58.00	24.80	16.37	57.00	24.41
Qwen2-VL-72B-Instruct	19.83	35.00	24.20	25.58	46.00	31.67	21.66	35.00	25.34	46.50	51.50	46.84
Qwen2-VL-7B-Instruct	9.99	20.00	12.67	15.57	32.00	20.04	8.99	17.00	11.17	30.66	47.50	34.30

Table 18: Performance of MLLMs on irregular multivariate time series anomalies ($r = 20\%$)

Anomaly Metrics	Irr-Triangle			Irr-Square			Irr-Sawtooth			Irr-Random		
	P	R	F1									
GPT-4o	<u>25.68</u>	<u>54.00</u>	<u>31.00</u>	<u>67.14</u>	<u>77.32</u>	<u>69.96</u>	<u>27.90</u>	<u>58.59</u>	<u>34.60</u>	94.58	94.89	94.32
GPT-4o-mini	9.41	33.50	14.22	14.06	50.50	21.09	9.07	35.00	14.03	24.40	59.00	32.48
Gemini-1.5-Pro	41.33	37.50	38.24	83.22	84.00	82.73	51.50	44.50	46.57	<u>89.50</u>	<u>88.50</u>	<u>88.83</u>
Gemini-1.5-Flash	8.00	8.00	7.40	34.18	40.00	35.56	5.33	5.50	4.84	<u>68.67</u>	<u>67.00</u>	<u>66.40</u>
LLaVA-NeXT-72B	17.54	75.77	27.10	16.29	69.90	25.18	18.88	72.92	28.13	14.61	56.32	21.79
LLaVA-NeXT-8B	15.72	52.53	23.17	14.65	51.50	22.04	15.46	55.00	23.18	15.27	49.50	22.46
Qwen2-VL-72B-Instruct	19.49	36.50	24.20	25.91	51.00	32.77	18.82	34.00	23.30	48.25	53.00	48.37
Qwen2-VL-7B-Instruct	12.33	25.00	16.00	15.45	34.50	20.72	10.33	22.50	13.80	23.37	41.50	27.36

Table 19: Performance of MLLMs on irregular multivariate time series anomalies ($r = 25\%$)

Anomaly Metrics	Irr-Triangle			Irr-Square			Irr-Sawtooth			Irr-Random		
	P	R	F1									
GPT-4o	30.67	46.88	32.11	<u>81.34</u>	<u>84.38</u>	<u>81.84</u>	<u>22.02</u>	45.00	26.15	97.46	97.83	97.25
GPT-4o-mini	6.43	23.50	9.77	17.35	57.58	25.20	5.84	22.00	8.96	23.45	58.00	31.17
Gemini-1.5-Pro	<u>27.83</u>	24.00	24.94	83.14	84.50	83.36	39.67	30.50	33.31	<u>90.50</u>	<u>90.50</u>	<u>90.23</u>
Gemini-1.5-Flash	6.17	4.50	4.80	29.09	31.50	29.23	4.00	3.00	3.33	74.72	70.00	70.40
LLaVA-NeXT-72B	15.57	66.50	23.84	16.88	68.04	25.19	13.94	65.82	21.99	18.43	68.37	26.95
LLaVA-NeXT-8B	17.66	<u>59.50</u>	<u>25.90</u>	16.44	54.55	24.02	14.74	<u>49.00</u>	21.58	16.26	51.50	23.65
Qwen2-VL-72B-Instruct	19.99	36.00	24.74	31.05	53.50	37.27	20.99	39.00	<u>26.27</u>	45.83	51.50	47.14
Qwen2-VL-7B-Instruct	12.33	24.50	16.00	16.11	33.50	21.02	11.99	26.00	16.00	22.82	43.00	27.70

Table 20: Performance of MLLMs on irregular Symbols time series anomalies ($r = 5\%$)

Anomaly Metrics	Irr-Global			Irr-Trend			Irr-Shaplet		
	P	R	F1	P	R	F1	P	R	F1
GPT-4o	36.74	11.66	14.08	50.49	43.74	45.09	49.44	52.74	49.29
GPT-4o-mini	<u>49.89</u>	<u>16.35</u>	23.65	53.53	59.59	53.68	49.76	73.99	58.17
Gemini-1.5-Pro	45.78	7.74	12.55	45.59	41.03	41.75	48.20	55.55	49.68
Gemini-1.5-Flash	46.33	6.51	11.08	48.50	41.94	43.60	46.02	52.70	47.59
LLaVA-NeXT-72B	51.53	10.89	17.67	60.52	61.73	59.05	59.02	61.88	59.03
LLaVA-NeXT-8B	47.72	16.14	<u>23.69</u>	11.46	17.48	13.69	15.25	26.51	19.23
Qwen2-VL-72B-Instruct	49.55	22.37	27.29	86.62	82.84	82.56	88.96	90.38	88.63
Qwen2-VL-7B-Instruct	46.62	9.18	15.05	<u>67.62</u>	<u>80.35</u>	<u>72.26</u>	<u>69.46</u>	<u>78.48</u>	<u>72.85</u>

Table 21: Performance of MLLMs on irregular Symbols time series anomalies ($r = 10\%$)

Anomaly Metrics	Irr-Global			Irr-Trend			Irr-Shaplet		
	P	R	F1	P	R	F1	P	R	F1
GPT-4o	52.98	26.74	30.07	82.85	86.77	82.94	79.52	77.43	76.44
GPT-4o-mini	31.27	5.73	9.59	44.01	68.65	52.37	56.07	74.34	61.74
Gemini-1.5-Pro	65.93	41.35	50.16	<u>89.74</u>	<u>87.20</u>	<u>86.33</u>	94.22	<u>92.96</u>	<u>92.56</u>
Gemini-1.5-Flash	<u>62.40</u>	<u>41.33</u>	<u>49.10</u>	90.74	96.56	92.99	<u>91.75</u>	95.51	92.93
LLaVA-NeXT-72B	48.89	12.20	18.86	61.43	64.75	61.17	57.44	59.68	56.66
LLaVA-NeXT-8B	49.72	16.04	23.80	12.31	22.03	15.66	21.15	28.74	23.80
Qwen2-VL-72B-Instruct	50.18	20.46	26.19	88.56	84.20	84.31	89.46	89.51	88.39
Qwen2-VL-7B-Instruct	45.68	9.19	14.98	69.25	82.19	73.91	69.27	77.21	72.22

Table 22: Performance of MLLMs on irregular Symbols time series anomalies ($r = 15\%$)

Anomaly Metrics	Irr-Global			Irr-Trend			Irr-Shaplet		
	P	R	F1	P	R	F1	P	R	F1
GPT-4o	27.91	7.77	9.12	49.71	43.10	44.77	47.93	61.67	52.57
GPT-4o-mini	<u>50.86</u>	18.37	25.08	51.72	61.76	53.70	50.70	<u>84.27</u>	62.69
Gemini-1.5-Pro	46.24	7.89	12.73	46.95	40.99	42.17	48.13	55.66	49.31
Gemini-1.5-Flash	33.36	4.85	8.01	45.58	41.31	41.96	32.44	47.62	37.62
LLaVA-NeXT-72B	49.52	10.84	17.28	62.31	63.06	60.70	60.48	64.04	60.16
LLaVA-NeXT-8B	48.30	16.27	23.74	17.65	33.30	23.02	21.63	35.53	26.40
Qwen2-VL-72B-Instruct	53.57	<u>17.99</u>	<u>24.92</u>	87.03	82.62	82.86	88.85	88.75	87.67
Qwen2-VL-7B-Instruct	45.62	9.59	15.39	<u>66.91</u>	<u>79.62</u>	<u>71.40</u>	<u>68.91</u>	76.53	<u>71.65</u>

Table 23: Performance of MLLMs on irregular Symbols time series anomalies ($r = 20\%$)

Anomaly Metrics	Irr-Global			Irr-Trend			Irr-Shaplet		
	P	R	F1	P	R	F1	P	R	F1
GPT-4o	26.31	5.72	8.27	48.80	41.19	43.12	39.50	53.27	43.77
GPT-4o-mini	<u>49.39</u>	<u>17.32</u>	<u>24.54</u>	49.71	61.49	52.20	49.51	<u>84.82</u>	61.94
Gemini-1.5-Pro	45.96	6.57	11.17	45.92	40.77	41.81	38.02	42.76	38.12
Gemini-1.5-Flash	34.79	4.61	7.93	45.97	41.72	42.30	26.25	44.96	32.56
LLaVA-NeXT-72B	46.52	12.24	18.27	61.65	63.26	60.30	57.95	64.14	59.38
LLaVA-NeXT-8B	47.26	16.12	23.28	12.74	21.65	15.59	27.34	35.61	28.78
Qwen2-VL-72B-Instruct	53.29	17.59	24.68	88.64	83.47	83.88	89.80	87.97	87.59
Qwen2-VL-7B-Instruct	46.70	10.43	16.33	<u>67.38</u>	<u>79.99</u>	<u>71.99</u>	<u>67.50</u>	76.66	<u>70.91</u>

Table 24: Performance of MLLMs on irregular Symbols time series anomalies ($r = 25\%$)

Anomaly Metrics	Irr-Global			Irr-Trend			Irr-Shaplet		
	P	R	F1	P	R	F1	P	R	F1
GPT-4o	24.92	5.10	7.49	47.56	41.80	42.94	40.94	54.01	45.01
GPT-4o-mini	48.60	17.99	25.09	49.61	62.10	52.46	50.13	88.60	63.74
Gemini-1.5-Pro	42.57	6.43	10.84	46.58	41.16	42.12	27.42	26.11	25.07
Gemini-1.5-Flash	34.73	4.96	8.42	45.44	40.54	41.26	32.96	59.84	41.84
LLaVA-NeXT-72B	<u>51.38</u>	11.79	18.36	62.58	61.73	60.19	57.39	64.40	58.96
LLaVA-NeXT-8B	48.91	16.14	<u>23.63</u>	16.92	28.36	20.87	15.89	28.91	20.42
Qwen2-VL-72B-Instruct	53.20	<u>16.76</u>	23.53	88.70	81.48	82.77	88.53	<u>84.60</u>	85.05
Qwen2-VL-7B-Instruct	47.51	10.64	16.69	<u>67.05</u>	<u>79.25</u>	<u>71.42</u>	<u>66.50</u>	74.50	<u>69.47</u>

Table 25: Performance of MLLMs on ArticulatoryWordRecognition time series anomalies ($M = 4$)

Anomaly Metrics	Triangle			Square			Sawtooth			Random		
	P	R	F1	P	R	F1	P	R	F1	P	R	F1
GPT-4o	<u>31.55</u>	43.88	<u>35.28</u>	85.17	100.00	89.73	40.56	59.18	46.13	24.83	42.86	30.25
GPT-4o-mini	23.23	72.00	34.94	31.04	<u>93.94</u>	46.27	25.57	<u>81.00</u>	38.67	20.24	<u>63.00</u>	30.44
Gemini-1.5-Pro	40.50	43.00	41.34	<u>80.92</u>	90.00	<u>83.74</u>	77.83	84.00	79.84	12.92	17.00	14.07
Gemini-1.5-Flash	15.17	20.00	16.67	72.33	82.00	75.51	<u>53.00</u>	62.00	<u>56.01</u>	10.67	15.00	12.00
LLaVA-NeXT-72B	22.89	<u>66.67</u>	33.21	23.47	72.45	34.56	23.06	66.67	33.37	<u>24.66</u>	72.73	35.90
LLaVA-NeXT-8B	25.33	44.00	31.18	24.91	47.00	31.51	29.33	53.00	36.98	19.58	40.00	25.71
Qwen2-VL-72B-Instruct	19.50	29.00	22.30	26.00	46.00	31.61	30.41	50.00	36.21	15.83	27.00	18.74
Qwen2-VL-7B-Instruct	19.07	52.00	27.64	21.16	64.00	31.34	24.49	71.00	35.94	23.24	<u>63.00</u>	<u>33.41</u>

Table 26: Performance of MLLMs on ArticulatoryWordRecognition time series anomalies ($M = 9$)

Anomaly Metrics	Triangle			Square			Sawtooth			Random		
	P	R	F1									
GPT-4o	46.99	<u>72.22</u>	54.59	<u>81.93</u>	<u>95.26</u>	<u>86.18</u>	43.54	61.22	48.54	<u>23.05</u>	41.00	27.64
GPT-4o-mini	18.19	71.00	28.35	19.23	67.35	29.08	17.13	66.50	26.56	16.78	66.50	26.15
Gemini-1.5-Pro	60.92	83.00	66.81	87.92	96.00	90.34	73.09	93.50	79.17	13.66	23.50	16.37
Gemini-1.5-Flash	<u>51.86</u>	69.00	<u>55.87</u>	70.26	84.50	75.15	<u>67.42</u>	<u>87.00</u>	<u>73.44</u>	23.83	29.50	24.82
LLaVA-NeXT-72B	19.10	65.00	28.01	16.34	69.19	25.06	15.58	64.95	23.74	18.01	<u>65.66</u>	<u>26.86</u>
LLaVA-NeXT-8B	16.05	34.00	21.14	17.87	41.50	24.14	15.80	37.00	21.29	17.26	38.50	22.85
Qwen2-VL-72B-Instruct	18.47	37.50	23.45	23.69	45.50	29.90	22.10	43.00	27.93	12.93	26.50	16.54
Qwen2-VL-7B-Instruct	19.32	35.50	24.50	19.32	35.50	24.50	19.32	35.50	24.50	19.32	35.50	24.50

Table 27: Performance of MLLMs on ArticulatoryWordRecognition time series anomalies ($M = 16$)

Anomaly Metrics	Triangle			Square			Sawtooth			Random		
	P	R	F1									
GPT-4o	<u>26.84</u>	45.75	<u>31.46</u>	<u>49.78</u>	60.89	<u>53.75</u>	28.08	42.26	32.34	<u>19.25</u>	37.75	22.39
GPT-4o-mini	11.45	46.50	17.57	16.11	58.50	24.38	12.80	48.83	19.67	11.51	46.80	17.74
Gemini-1.5-Pro	45.11	74.17	52.20	63.54	81.67	69.06	52.43	81.50	59.44	19.75	44.16	24.57
Gemini-1.5-Flash	24.40	50.50	30.74	34.80	49.83	39.14	<u>28.23</u>	51.66	<u>33.93</u>	17.36	41.16	<u>22.67</u>
LLaVA-NeXT-72B	12.46	<u>70.33</u>	19.98	12.21	<u>66.67</u>	19.46	11.47	<u>63.66</u>	18.01	13.46	70.58	20.79
LLaVA-NeXT-8B	11.48	26.83	15.15	12.28	27.00	16.11	12.52	27.16	15.92	13.39	33.83	18.12
Qwen2-VL-72B-Instruct	16.97	54.50	24.71	19.56	59.67	27.96	16.58	55.50	24.31	14.95	<u>52.50</u>	21.47
Qwen2-VL-7B-Instruct	11.73	19.00	13.26	11.99	19.00	13.63	12.12	20.00	14.03	11.66	16.49	13.10

Table 28: Performance of MLLMs on ArticulatoryWordRecognition time series anomalies ($M = 25$)

Anomaly Metrics	Triangle			Square			Sawtooth			Random		
	P	R	F1									
GPT-4o	21.40	42.28	25.87	30.86	39.93	33.90	21.69	34.86	24.88	10.56	35.97	15.10
GPT-4o-mini	9.14	37.71	14.00	11.11	38.69	16.57	8.88	33.67	13.21	9.74	41.67	14.84
Gemini-1.5-Pro	33.21	47.17	36.10	50.36	58.67	52.65	44.20	<u>60.83</u>	47.87	6.53	13.17	7.86
Gemini-1.5-Flash	<u>28.45</u>	39.83	<u>30.19</u>	<u>32.95</u>	39.08	<u>34.81</u>	<u>29.72</u>	35.67	<u>29.54</u>	17.22	38.08	20.08
LLaVA-NeXT-72B	9.98	<u>64.18</u>	15.50	9.84	<u>66.84</u>	15.52	9.16	58.50	14.04	9.37	<u>62.32</u>	15.22
LLaVA-NeXT-8B	8.27	36.00	12.61	9.97	37.58	14.39	8.87	37.91	13.21	<u>11.67</u>	41.66	<u>16.76</u>
Qwen2-VL-72B-Instruct	8.91	53.00	14.31	10.70	60.92	17.08	9.94	54.59	15.68	8.94	46.75	13.06
Qwen2-VL-7B-Instruct	11.88	85.91	18.43	11.44	88.67	18.32	11.38	85.58	18.24	10.11	85.50	16.61

Table 29: Performance of MLLMs on ArticulatoryWordRecognition time series anomalies ($M = 36$)

Anomaly Metrics	Triangle			Square			Sawtooth			Random		
	P	R	F1									
GPT-4o	19.94	29.47	22.34	<u>22.75</u>	28.09	<u>24.57</u>	<u>20.01</u>	25.30	<u>21.39</u>	11.40	41.24	16.04
GPT-4o-mini	8.81	31.06	12.88	9.21	32.22	13.72	7.93	26.51	11.67	7.11	27.73	10.77
Gemini-1.5-Pro	<u>17.35</u>	39.42	<u>21.61</u>	26.49	32.68	27.83	21.08	40.80	25.83	<u>9.68</u>	25.79	11.70
Gemini-1.5-Flash	14.96	27.45	17.53	19.19	23.53	20.26	18.00	26.65	19.96	7.84	21.82	10.58
LLaVA-NeXT-72B	8.63	<u>67.93</u>	13.85	8.76	<u>69.06</u>	14.59	7.38	<u>65.47</u>	12.56	7.79	<u>61.96</u>	12.72
LLaVA-NeXT-8B	9.03	35.53	13.20	8.82	33.22	12.72	8.34	34.08	12.23	9.37	36.03	13.45
Qwen2-VL-72B-Instruct	9.03	50.40	13.69	9.43	53.48	14.77	9.37	43.30	13.90	9.41	40.32	<u>13.80</u>
Qwen2-VL-7B-Instruct	8.36	85.05	14.33	7.47	87.13	13.53	7.51	86.73	13.61	7.01	83.05	12.71

Table 30: Performance of MLLMs on irregular ArticulatoryWordRecognition time series anomalies ($r = 5\%$)

Anomaly Metrics	Irr-Triangle			Irr-Square			Irr-Sawtooth			Irr-Random		
	P	R	F1									
GPT-4o	37.67	64.80	45.28	<u>78.09</u>	96.94	<u>83.71</u>	53.99	85.20	63.53	<u>19.95</u>	37.76	23.86
GPT-4o-mini	17.30	69.50	27.04	18.47	69.70	28.38	17.00	72.00	26.89	15.82	<u>64.00</u>	24.69
Gemini-1.5-Pro	52.73	79.50	59.75	81.13	<u>96.00</u>	85.48	<u>70.40</u>	97.50	78.11	16.41	28.50	19.74
Gemini-1.5-Flash	<u>46.64</u>	<u>72.50</u>	<u>53.11</u>	70.84	86.50	76.04	72.17	<u>87.00</u>	<u>74.71</u>	21.28	28.50	22.60
LLaVA-NeXT-72B	18.15	67.53	27.01	14.89	68.00	23.30	16.32	62.50	24.13	14.16	66.84	22.37
LLaVA-NeXT-8B	15.28	43.50	21.77	15.40	40.50	21.41	18.53	48.00	25.78	15.33	42.50	21.48
Qwen2-VL-72B-Instruct	16.05	37.00	21.11	21.09	53.50	28.61	20.98	45.00	27.22	11.85	28.50	16.16
Qwen2-VL-7B-Instruct	17.99	38.50	23.90	17.99	38.50	23.90	17.99	38.50	23.90	17.99	38.50	<u>23.90</u>

Table 31: Performance of MLLMs on irregular ArticulatoryWordRecognition time series anomalies ($r = 10\%$)

Anomaly Metrics	Irr-Triangle			Irr-Square			Irr-Sawtooth			Irr-Random		
	P	R	F1									
GPT-4o	42.54	76.80	52.13	62.94	<u>90.91</u>	71.26	51.94	84.00	61.09	<u>20.26</u>	40.82	<u>25.64</u>
GPT-4o-mini	17.31	72.50	27.33	19.23	74.24	29.78	17.40	72.50	27.37	16.92	71.72	26.77
Gemini-1.5-Pro	56.28	91.00	66.16	81.57	98.00	86.74	<u>65.13</u>	97.00	<u>74.45</u>	13.18	25.00	16.14
Gemini-1.5-Flash	<u>49.75</u>	<u>78.00</u>	<u>56.98</u>	<u>67.75</u>	86.00	<u>73.84</u>	71.53	<u>89.50</u>	75.93	20.73	30.00	23.06
LLaVA-NeXT-72B	15.46	60.50	23.31	14.76	64.43	22.87	16.04	63.40	24.38	15.07	<u>66.67</u>	23.42
LLaVA-NeXT-8B	17.25	45.00	24.00	17.44	46.50	24.55	16.16	46.50	23.28	18.64	44.50	25.39
Qwen2-VL-72B-Instruct	16.16	39.00	21.88	26.19	60.00	34.71	19.51	44.00	25.96	10.76	25.00	14.36
Qwen2-VL-7B-Instruct	17.99	38.50	23.90	17.99	38.50	23.90	17.99	38.50	23.90	17.99	38.50	23.90

Table 32: Performance of MLLMs on irregular ArticulatoryWordRecognition time series anomalies ($r = 15\%$)

Anomaly Metrics	Irr-Triangle			Irr-Square			Irr-Sawtooth			Irr-Random		
	P	R	F1									
GPT-4o	47.42	<u>87.11</u>	58.57	61.30	<u>96.50</u>	71.68	54.32	<u>93.75</u>	65.21	22.87	48.97	29.85
GPT-4o-mini	17.19	74.50	27.33	18.27	73.50	28.68	18.31	75.00	28.79	15.56	<u>65.00</u>	<u>24.57</u>
Gemini-1.5-Pro	56.06	92.50	66.65	73.57	98.00	81.28	<u>61.21</u>	96.00	<u>71.65</u>	14.19	26.00	17.12
Gemini-1.5-Flash	<u>53.57</u>	84.00	<u>61.71</u>	<u>65.19</u>	87.00	<u>72.16</u>	68.74	89.00	74.62	<u>19.87</u>	35.50	23.73
LLaVA-NeXT-72B	14.72	62.24	22.49	15.75	66.16	23.78	14.03	61.73	21.63	15.88	66.67	24.32
LLaVA-NeXT-8B	18.79	47.50	25.86	17.43	45.00	24.12	16.53	41.00	22.55	17.16	44.00	23.82
Qwen2-VL-72B-Instruct	17.35	38.00	22.85	24.99	54.50	32.53	20.30	45.00	26.91	11.98	26.50	15.87
Qwen2-VL-7B-Instruct	17.99	38.50	23.90	18.11	39.50	24.12	17.99	38.50	23.90	17.99	38.50	23.90

Table 33: Performance of MLLMs on irregular ArticulatoryWordRecognition time series anomalies ($r = 20\%$)

Anomaly Metrics	Irr-Triangle			Irr-Square			Irr-Sawtooth			Irr-Random		
	P	R	F1									
GPT-4o	47.51	89.18	58.76	56.47	<u>94.15</u>	67.01	49.93	<u>95.45</u>	62.48	22.23	51.55	29.18
GPT-4o-mini	17.38	76.00	27.64	17.30	69.50	27.13	18.55	77.50	29.33	16.22	<u>68.50</u>	25.69
Gemini-1.5-Pro	56.33	94.50	68.14	70.17	98.50	78.94	<u>59.58</u>	95.50	70.34	17.15	30.50	21.01
Gemini-1.5-Flash	<u>54.68</u>	<u>89.50</u>	<u>64.49</u>	<u>60.88</u>	88.00	<u>68.93</u>	64.92	85.50	<u>70.25</u>	<u>19.71</u>	36.00	23.29
LLaVA-NeXT-72B	16.83	69.39	25.72	16.65	65.98	25.05	17.30	69.00	26.30	18.53	71.43	<u>27.53</u>
LLaVA-NeXT-8B	17.89	46.00	24.68	16.44	43.00	22.92	15.91	43.50	22.43	16.79	42.50	23.15
Qwen2-VL-72B-Instruct	17.38	39.00	23.27	27.61	58.00	36.14	17.31	38.00	22.77	13.54	29.50	17.84
Qwen2-VL-7B-Instruct	17.99	38.50	23.90	18.11	39.50	24.12	17.99	38.50	23.90	17.99	38.50	23.90

Table 34: Performance of MLLMs on irregular ArticulatoryWordRecognition time series anomalies ($r = 25\%$)

Anomaly Metrics	Irr-Triangle			Irr-Square			Irr-Sawtooth			Irr-Random		
	P	R	F1									
GPT-4o	46.22	95.83	59.96	46.91	<u>94.27</u>	59.91	44.98	<u>95.26</u>	58.45	<u>21.11</u>	54.08	29.04
GPT-4o-mini	17.92	75.25	28.40	19.28	77.00	30.12	17.90	74.50	28.27	17.86	75.00	<u>28.34</u>
Gemini-1.5-Pro	56.31	<u>93.00</u>	67.31	<u>61.58</u>	97.50	72.31	<u>59.20</u>	97.00	<u>70.08</u>	18.70	33.50	22.56
Gemini-1.5-Flash	<u>55.51</u>	89.00	<u>64.96</u>	62.77	88.50	<u>70.77</u>	65.89	91.00	73.47	21.41	45.50	26.75
LLaVA-NeXT-72B	16.92	65.82	25.31	18.67	75.25	28.37	18.58	70.50	27.42	14.88	<u>57.07</u>	22.14
LLaVA-NeXT-8B	15.34	41.50	21.49	15.81	42.50	22.11	17.23	42.50	23.62	15.43	39.50	21.10
Qwen2-VL-72B-Instruct	19.78	46.00	26.82	26.04	57.00	34.24	22.23	50.00	29.73	11.48	25.00	15.11
Qwen2-VL-7B-Instruct	17.99	38.50	23.90	18.24	40.50	24.34	18.11	39.50	24.12	17.99	38.50	23.90